

UCSF

UC San Francisco Previously Published Works

Title

CD3 ζ adaptor structure determines functional differences between human and mouse CD16 Fc-gamma receptor signaling in natural killer cells

Permalink

<https://escholarship.org/uc/item/5jv544cg>

Journal

The Journal of Immunology, 208(1_Supplement)

ISSN

0022-1767

Authors

Aguilar, Oscar A
Fong, Lam-Kiu
Ishiyama, Kenichi
[et al.](#)

Publication Date

2022-05-01

DOI

10.4049/jimmunol.208.suppl.164.04

Peer reviewed

ARTICLE

Diminished cell proliferation promotes natural killer cell adaptive-like phenotype by limiting FcεR1y expression

Avishai Shemesh^{1,2}, Yapeng Su³, Daniel R. Calabrese^{4,5}, Daniel Chen^{3,6,7}, Janice Arakawa-Hoyt¹, Kole T. Roybal^{1,2,8,9,10,11}, James R. Heath^{3,12}, John R. Greenland^{4,5}, and Lewis L. Lanier^{1,2}

Human adaptive-like natural killer (NK) cells express low levels of FcεR1y (FcRy^{-/low}) and are reported to accumulate during COVID-19 infection; however, the mechanism underlying and regulating FcRy expression in NK cells has yet to be fully defined. We observed lower FcRy protein expression in NK cell subsets from lung transplant patients during rapamycin treatment, suggesting a link with reduced mTOR activity. Further, FcRy^{-/low} NK cell subsets from healthy donors displayed reduced mTOR activity. We discovered that FcRy upregulation is dependent on cell proliferation progression mediated by IL-2, IL-15, or IL-12, is sensitive to mTOR suppression, and is inhibited by TGFβ or IFNα. Accordingly, the accumulation of adaptive-like FcRy^{-/low} NK cells in COVID-19 patients corresponded to increased TGFβ and IFNα levels and disease severity. Our results show that an adaptive-like NK cell phenotype is induced by diminished cell proliferation and has an early prognostic value for increased TGFβ and IFNα levels in COVID-19 infection associated with disease severity.

Introduction

NK cells are innate lymphocytes with adaptive features, functionally regulated by activating and inhibitory germline-encoded receptors (Cerwenka and Lanier, 2016; Sun et al., 2009; Schlums et al., 2015). The adaptor FcRy is encoded by the FCER1G gene and forms homodimers or heterodimers with the adaptor CD3ζ. These adaptor dimers assemble a molecular complex with the activating receptors CD16 (FcγRIII), NKp30, or NKp46 on the cell surface of human NK cells (Lanier, 2009; Liu et al., 2020). Human peripheral blood immature NK cells (CD3⁺CD56^{bright}CD16⁻NKG2A⁺) express low FcRy levels, whereas mature NK cells (CD3⁺CD56^{dim}CD16⁺NKG2A[±]) show increased FcRy expression (Cooper et al., 2001; Björkström et al., 2010; Lopez-Vergès et al., 2010). A subset of mature NK cells designated adaptive NK cells is characterized by low or negative FcRy expression and reduced expression of PLZF, Siglec-7, Syk, CD161, NKG2A, NKp30, and NKp46 (Schlums et al., 2015; Lee et al., 2015). CRISPR knockout of the FCER1G gene induces adaptive-like features in human NK cells (Liu et al., 2020). Adaptive or adaptive-like FcRy^{-/low} NK cells are found in healthy

individuals' peripheral blood and solid tissues including the lung and exhibit stable long-term population frequencies (Muccio et al., 2018; Brownlie et al., 2021).

The expansion of adaptive FcRy^{-/low} NK cells is associated with human cytomegalovirus (HCMV) infection and higher expression of the activating receptor CD94-NKG2C (Schlums et al., 2015; Brownlie et al., 2021; Lee et al., 2015). However, the adaptive NK cell phenotype is not confined to NKG2C-expressing cells alone, and the stimuli driving their differentiation are unknown (Liu et al., 2016). In vivo, anti-HCMV antibody titers and HCMV UL40 peptide-induced CD94-NKG2C-dependent NK cell activation correlate with increased frequencies of adaptive NK cells in HCMV-infected individuals (Lee et al., 2015; Rölle et al., 2018; Wu et al., 2013). Ex vivo CD16 stimulation is suggested to expand adaptive FcRy^{-/low} cells relative to nonadaptive FcRy^{high} NK cells due to the CD16 transmembrane domain interaction with CD3ζ homodimers (Schlums et al., 2015; Lee et al., 2015; Liu et al., 2020; Lanier et al., 1991). Adaptive or adaptive-like NK cells alter the risk for myeloma

¹Department of Microbiology and Immunology, University of California, San Francisco, San Francisco, CA; ²Parker Institute for Cancer Immunotherapy, University of California, San Francisco, San Francisco, CA; ³Institute for Systems Biology, Seattle, WA; ⁴Department of Medicine, University of California, San Francisco, CA; ⁵Medical Service, Veterans Affairs Health Care System, San Francisco, CA; ⁶Department of Microbiology, University of Washington, Seattle, WA; ⁷Department of Informatics, University of Washington, Seattle, WA; ⁸Helen Diller Family Comprehensive Cancer Center, University of California, San Francisco, San Francisco, CA; ⁹Chan Zuckerberg Biohub, San Francisco, CA; ¹⁰Gladstone University of California, San Francisco Institute for Genetic Immunology, San Francisco, CA; ¹¹University of California, San Francisco Cell Design Institute, San Francisco, CA; ¹²Department of Bioengineering, University of Washington, Seattle, WA.

Correspondence to Avishai Shemesh: avishaih83@gmail.com; Lewis L. Lanier: lewis.lanier@ucsf.edu.

© 2022 Shemesh et al. This article is distributed under the terms of an Attribution–Noncommercial–Share Alike–No Mirror Sites license for the first six months after the publication date (see <http://www.rupress.org/terms/>). After six months it is available under a Creative Commons License (Attribution–Noncommercial–Share Alike 4.0 International license, as described at <https://creativecommons.org/licenses/by-nc-sa/4.0/>).

relapse (Zaghi et al., 2021; Merino et al., 2021), while in COVID-19 infection patients with poor outcomes display an adaptive NK cell expansion (Varchetta et al., 2021).

NK cell proliferation or expansion is regulated by IL-2, IL-15, and IL-12 (Wang and Zhao, 2021; Wiedemann et al., 2020; Shemesh et al., 2022), by the phosphorylation of STAT5 (pSTAT5), STAT4 (pSTAT4), and other STATs directly or indirectly, and by the activation of mammalian target of rapamycin (mTOR) complexes (Marçais et al., 2014; Anton et al., 2015; Anton et al., 2020). Activation of the mTOR complex-1 (mTORC1) leads to ribosomal protein S6 phosphorylation at position S235/236 (pS6^{S235/236}) and regulates cap-dependent protein translation and cell cycle progression (Marçais et al., 2014). The mTOR complex-2 (mTORC2) phosphorylates AKT at position S473 (pAKT^{S473}), which inhibits FOXO1 activity, a suppressor of cell cycle progression (Wang et al., 2018; Calnan and Brunet, 2008). TGFβ or IFNα can diminish NK cell proliferation by various signaling pathways with or without inhibition of mTOR activity (Platanias, 2005; Viel et al., 2016; Gartel and Tyner, 2002; Shemesh et al., 2022).

Here, we found a mechanism limiting FcRγ protein upregulation caused by diminished NK cell proliferation. Rapamycin treatment of lung transplant patients, low mTOR activity, and incubation of NK cells in the presence of rapamycin, TGFβ, or IFNα were, respectively, associated with lower FcRγ expression and an adaptive NK cell phenotype in healthy donors. Low FcRγ expression highly correlated with diminished cell proliferation. Additionally, we showed that during COVID-19 infection, NK cells with an adaptive-like phenotype increase in association with higher TGFβ and IFNα and disease severity. Our results suggest that alteration in signaling pathways leading to diminished NK cell proliferation support an adaptive-like NK cell phenotype. Further, in COVID-19 infection, early accumulation of adaptive-like NK cells can serve as an early prognostic biomarker associated with increased inflammation.

Results

Rapamycin treatment is associated with reduced FcRγ levels in NK cells from lung transplant patients

mTOR activity influences NK cell differentiation (Marçais et al., 2014; Yang et al., 2018). Rapamycin is an immune-suppressive agent used during solid organ transplantation with known mTOR selectivity (Sarbasov et al., 2006; Augustine et al., 2007; Calabrese et al., 2021). Therefore, we investigated if rapamycin treatment can alter the frequency of human NK cell subsets by comparing matched peripheral blood mononuclear cell (PBMC) samples obtained from lung transplant patients before and during rapamycin treatment (Fig. 1 A and Fig. S1 A). As a control comparison, we analyzed samples from lung transplant patients at least 1 yr after transplant while on standard immunosuppression but not rapamycin and matched for transplant indication. Using flow cytometry analysis, PBMCs were gated on live CD45⁺dump⁻ (CD3⁻CD19⁻CD14⁻CD123⁻CD4⁻) NKp46⁺, CD56⁺ lymphocytes to identify NK cells, and then subgated the NK cells into four subsets based on NKG2A and CD16 expression: immature NKG2A⁺CD16⁻, immature NKG2A⁺CD16^{low}, mature

NKG2A⁺CD16⁺, and mature NKG2A⁻CD16⁺ (Fig. S1 B). Additionally, we examined markers associated with NK cell differentiation (CD57, NKG2C, and FcRγ), proliferation (Ki-67), and mTORC1 activity (pS6^{S235/236}). The percentage of NK cells within the CD45⁺ population significantly increased during rapamycin treatment, possibly due to reduced T cell frequencies (Fig. S1 B). NK cell subset analysis showed a significant increase in mature NKG2A⁻CD16⁺ CD57⁺ cells (Fig. 1 B). NKG2C expression did not correlate with FcRγ expression levels (Fig. S1 C). All the defined NK cell subsets displayed significantly lower FcRγ levels during rapamycin treatment (Fig. 1 C and Fig. S1 D), accompanied by a lower percentage of Ki-67⁺ cells and relatively fewer pS6^{S235/236} cells (Fig. 1, D and E). Overall, the results show that rapamycin treatment is associated with reduced mTOR activity, decreased cell proliferation, and lower FcRγ expression in human NK cells.

FcRγ expression at steady state is associated with mTOR activity

In healthy donors (HDs), reduced FcRγ expression is reported in immature and mature adaptive NK cells compared with FcRγ levels in mature nonadaptive NK cells (Hart et al., 2019). To evaluate if reduced mTOR activity is associated with lower FcRγ expression, we analyzed FcRγ expression and mTORC1/C2 activity in steady-state (resting) NK cells by flow cytometry. Additionally, we examined IL-2 receptor chain expression and downstream STATs and PI3K signaling as IL-2 signaling can influence FcRγ expression and mTORC1/C2 activity (Pahl et al., 2018; Wang and Zhao, 2021).

NK cells were isolated by negative selection from peripheral blood to avoid inadvertent stimulation during cell processing (Fig. 2 A). HDs were grouped into adaptive NK cell-positive HDs (positive for mature NKG2A⁻NKG2C^{high}FcRγ⁻ or FcRγ^{low} NK cells, $n = 4$, all HCMV seropositive) or adaptive NK cell-negative HDs (negative for mature NKG2A⁺NKG2C⁺FcRγ^{-/low} NK cells [Liu et al., 2016], $n = 9$ [3 HCMV-seropositive, 6 HCMV-seronegative]; Fig. 2 A; and Fig. S2, A and B). In all HDs, immature CD56^{bright}CD16⁻ NK cells expressed low FcRγ levels (Fig. S2 A; Hart et al., 2019). Adaptive NK cell-positive HDs exhibited higher percentages of mature NKG2A⁻CD57⁺ cells, associated with NK cell maturation, relative to adaptive NK cell-negative HDs (Fig. S2 D; Björkström et al., 2010). Adaptive NK cells displayed reduced PLZF, Syk, CD161, Siglec-7, NKp30, and NKp46, while immature NK cells displayed a differential expression pattern with high levels of Syk, NKp30, NKp46, and CD25 (Fig. S3, A and B; Schlums et al., 2015; Lee et al., 2015).

Therefore, in adaptive NK cell-positive HDs, we compared cell signaling markers between immature CD56^{bright}CD16⁻ and mature CD56^{dim}CD16⁺ NK cells, further gated into the following subsets: nonadaptive NKG2A^{-/+}NKG2C⁻FcRγ^{high}, adaptive NKG2A⁻NKG2C^{high}FcRγ^{low}, and adaptive NKG2A⁻NKG2C^{high}FcRγ⁻, and between CD57⁻ and CD57⁺ cells within each of the defined mature subsets (Fig. 2 B). As a control, in adaptive NK cell-negative HDs, we examined the expression of signaling markers associated with NK cell maturation in the defined subsets: NKG2A⁺CD57⁻, NKG2A⁺CD57⁺, NKG2A⁻CD57⁻, and NKG2A⁻CD57⁺ (most mature; Fig. S2 D) to differentiate between

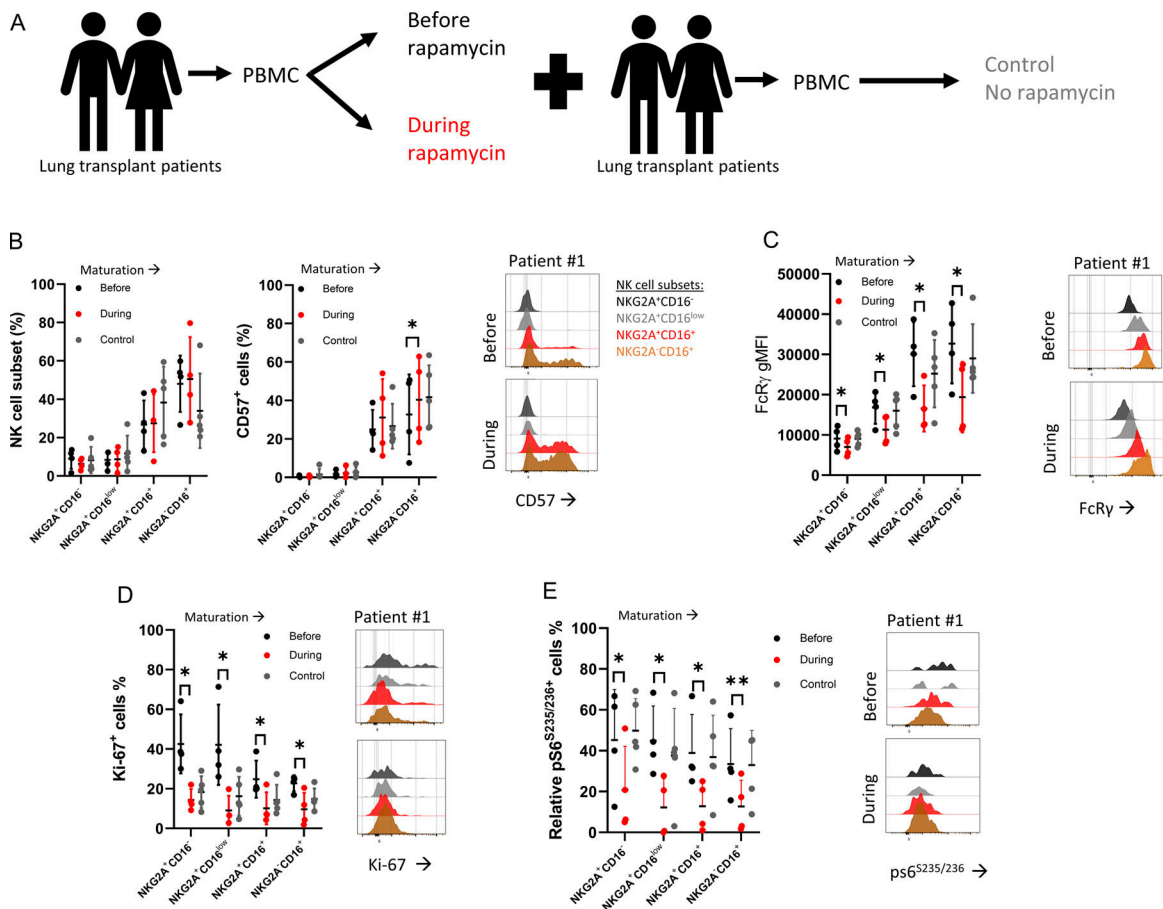


Figure 1. FcR γ levels in NK cells from lung transplant patients during rapamycin treatment. (A) Schematic of sample evaluation. PBMC samples from lung transplant recipients before or during rapamycin administration ($n = 4$) were assessed for NK cell subsets. Control group = patients at least 1-yr post-transplant and matched for transplant indication ($n = 5$). (B) Percentages of defined NK cell subsets and percentages of CD57 $^{+}$ cells. Right: Representative histograms of CD57 staining in the defined NK cell subsets (color-coded; NKG2A $^{+}$ CD16 $^{-}$ [black], NKG2A $^{+}$ CD16 low [gray], NKG2A $^{+}$ CD16 $^{+}$ [red], NKG2A $^{+}$ CD16 $^{+}$ [orange]) before and during rapamycin treatment. (C) FcR γ gMFI in the defined NK cell subsets, with representative histograms before and during rapamycin treatment in the defined NK cell subsets (color-coded). (D) Percentages of Ki-67 $^{+}$ NK cells in the defined NK cell subsets, with representative histograms before and during rapamycin treatment in the defined NK cell subsets (color-coded). (E) Relative pS6 $^{+}$ NK cells in the defined NK cell subsets, with representative histograms before and during rapamycin treatment in the defined NK cell subsets (color-coded). Statistical analysis was done between matched samples, mean \pm SD, paired t test, parametric. *, $P \leq 0.05$; **, $P < 0.01$.

adaptive-associated or maturation-associated cell signaling alterations (Björkström et al., 2010).

STATs phosphorylation, examined by pSTAT1 Y701 , pSTAT4 Y693 , or pSTAT5 Y694 expression levels (Wiedemann et al., 2021), were lower in the adaptive FcR γ^{-} or FcR γ^{low} subsets relative to nonadaptive mature NKG2C-FcR γ^{high} CD57 $^{-}$ NK cells (normalization index = 1), and increased in immature CD56 bright CD16 $^{-}$ FcR γ^{low} NK cells (Fig. 2 B and Fig. S3 B). In line with the lower STATs activity, CD122 expression decreased with the adaptive phenotype (Fig. 2 C). In HDs without adaptive NK cells STATs activity and CD122 expression were reduced with NK cell maturation relative to immature NK cells (Fig. 2, D and E). However, mature CD57 $^{+}$ cells exhibited increased STATs activity relative to mature CD57 $^{-}$ cells (Fig. 2 D) and further reduced CD122 levels. Yet these changes did not translate to changes in FcR γ levels (Fig. 2, E and F; Björkström et al., 2010). Therefore, we concluded that the reduced FcR γ expression is not

directly associated with reduced STATs activity or reduced CD122 expression in peripheral blood adaptive NK cells.

PI3K activity (pAKT T308 ; Mace, 2018) showed no significant differences between the defined adaptive NK cell subsets (Fig. 3 A and Fig. S3 B). However, mTOR activity measured by pS6 $^{S235/236}$ (mTORC1) or pAKT S473 (mTORC2; Wang and Zhao, 2021; Yang et al., 2015) was significantly lower in immature CD56 bright CD16 $^{-}$ NK cells and adaptive FcR γ^{low} or FcR γ^{-} NK cell subsets. Moreover, we detected reduced mTOR protein levels while Bcl2 expression was high in adaptive NK cells (Fig. 3 A; Barnes et al., 2020). In adaptive NK cell-negative donors, PI3K activity decreased with cell maturation (Fig. 3 B). mTOR activity (specifically mTORC2 [pAKT S473]) was lower in immature NK cells with no difference in mature NK cell subsets (Fig. 3 B). mTOR protein decreased with maturation, and Bcl2 expression increased (Fig. 3 B). These results indicated that the FcR $\gamma^{-/low}$ phenotype, observed in peripheral blood immature NK cells and

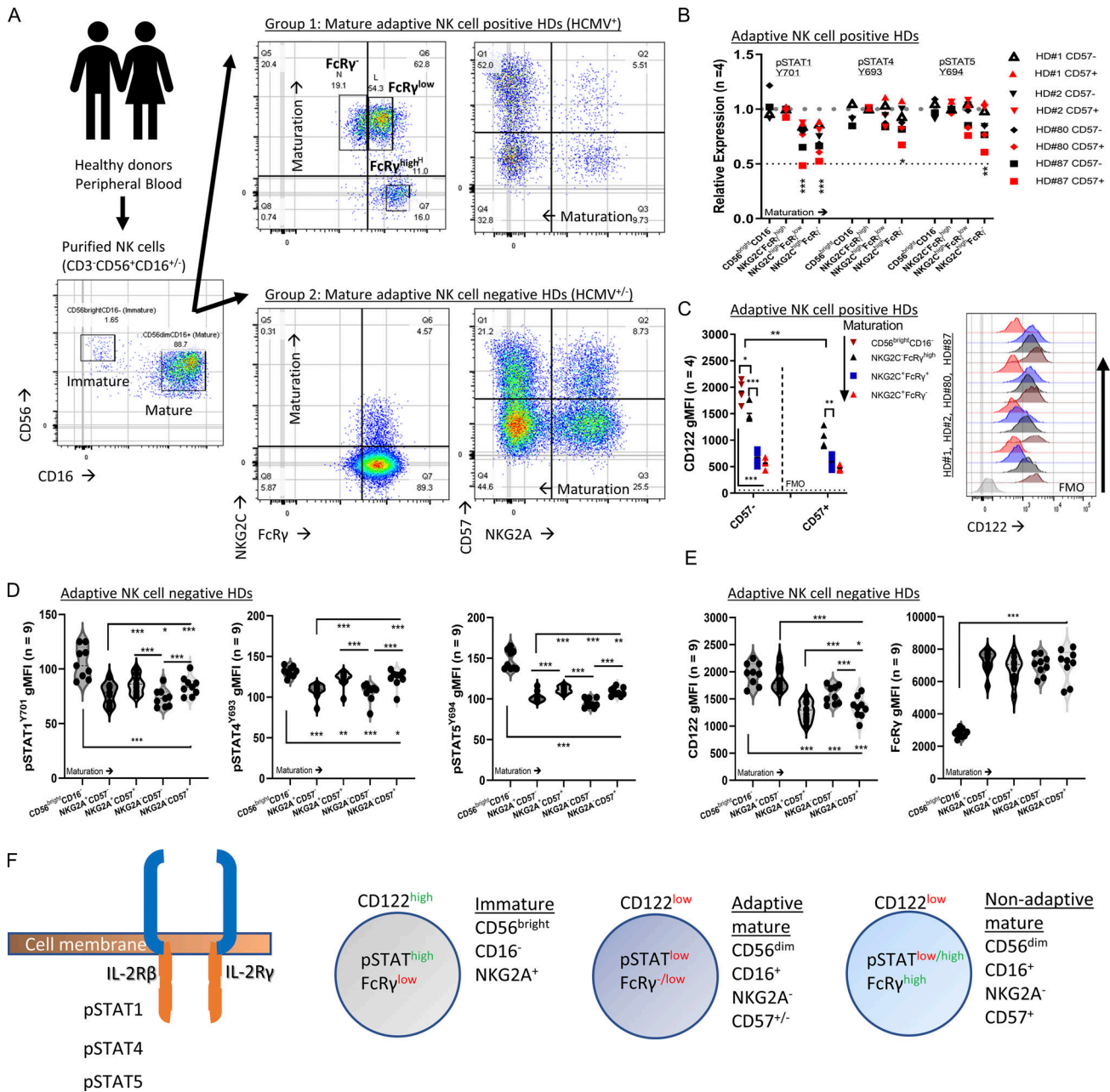


Figure 2. FcR γ expression at steady state is associated with mTOR activity. Purified primary NK cells were examined ex vivo, without additional stimulation, for the indicated markers. n = number of donors, paired t test, parametric. *, $P < 0.05$; **, $P < 0.01$; ***, $P < 0.001$. **(A)** Peripheral blood samples were obtained from healthy donors. NK cells (CD3⁺CD56⁺CD16⁺) were purified by negative selection from peripheral blood samples and classified into Group 1 (adaptive NK cell–positive HDs [#1, 2, 80, 87; HCMV-seropositive]) and Group 2 (adaptive NK cell–negative HDs [#77, 82, 86, 88, 89, 91, HCMV-seronegative; and 78, 84, 85, HCMV-seropositive]). Gating strategy: CD3⁺CD56⁺CD16⁺ NK cells were gated as immature CD56^{bright}CD16⁻ and mature CD56^{dim}CD16⁺. In adaptive NK cell–positive HDs, mature NK cells were examined for NKG2C and FcR γ expression and gated as NKG2C^{high}FcR γ ^{negative}, NKG2C^{high}FcR γ ^{low}, and NKG2A⁺NKG2C^{negative}FcR γ ^{high} NK cells. For NK cell maturation, NK cells were gated as NKG2A versus CD57. **(B)** Relative expression of phospho-STAT1^{Y701}, STAT4^{Y693}, and STAT5^{Y694} in the indicated NK cell subsets in adaptive NK cell–positive HDs from 4 HDs. The gMFI values were determined for the indicated NK cell subsets and were then normalized relative to the gMFI values measured for the mature nonadaptive NKG2C⁻FcR γ ^{high}CD57⁻ NK cells in the same donor, which were established as index = 1 (upper dashed line), index = 0.5 (lower dashed line). **(C)** Expression of CD122 in the indicated NK cell subsets in adaptive NK cell–positive HDs. Right: Histograms of CD122 expression per NK cell subset for each donor (color-coded; horizontal dashed line = FMO control values). **(D)** Expression of pSTAT1^{Y701}, pSTAT4^{Y693}, and pSTAT5^{Y694} in the indicated NK cell subsets in adaptive NK cell–negative HDs. Violin plots. **(E)** Expression of CD122 and FcR γ in the indicated NK cell subsets in adaptive NK cell–negative HDs. Violin plots. **(F)** Schematic of examined signaling and associated markers in the defined NK cells subsets.

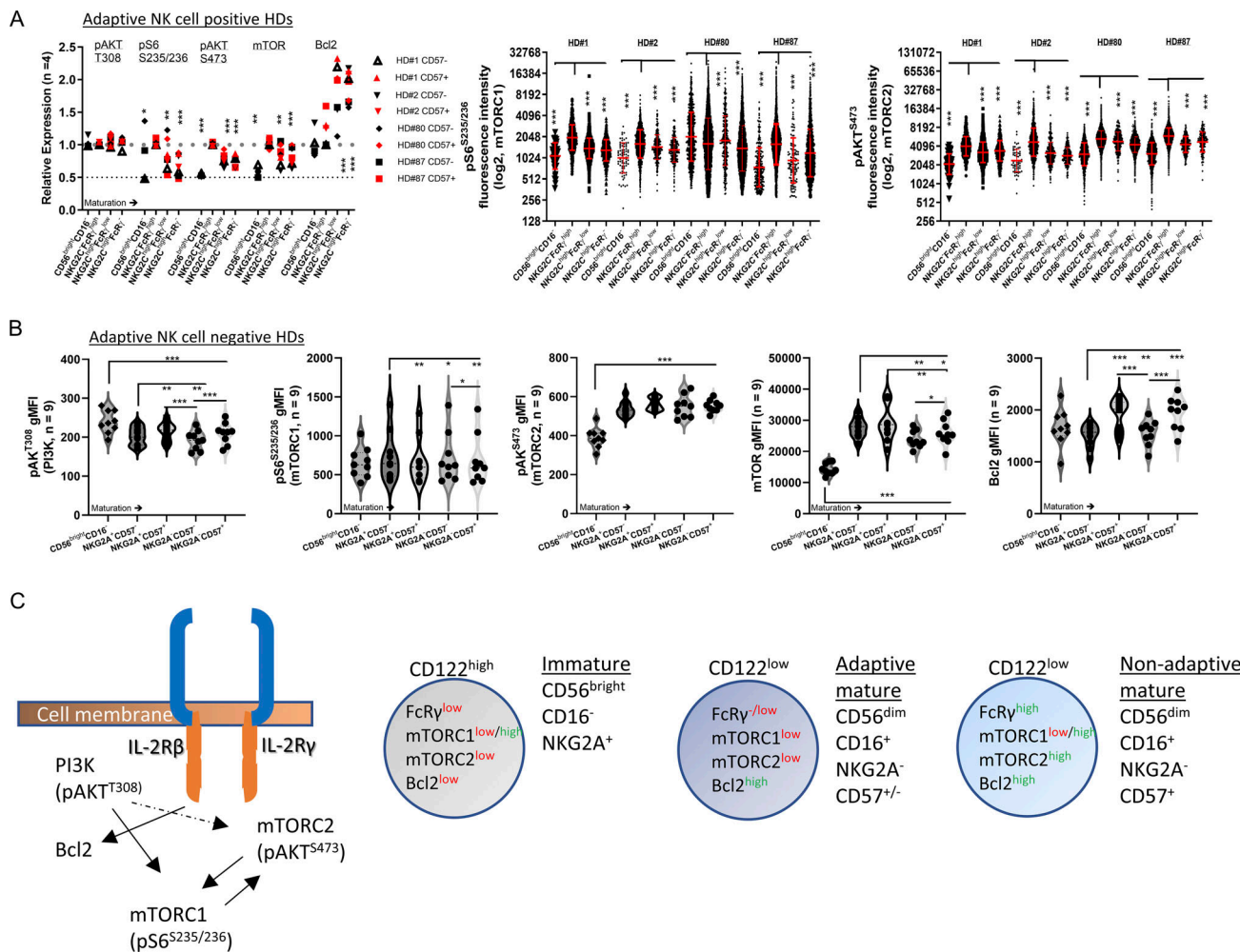


Figure 3. PI3K and mTOR activity in immature, mature, and adaptive NK cells. (A) Relative expression of pAKT^{T308} (PI3K activity), pS6^{S235/236} (mTORC1), pAKT^{S473} (mTORC2), mTOR protein, and Bcl2 protein in the indicated NK cell subsets in adaptive NK cell-positive HDs. Expression was normalized relative to NKG2C-FcRγ^{high}CD57⁻ cells that are index = 1 (upper dashed line), index = 0.5 (lower dashed line). Paired t test. *, P < 0.05; **, P < 0.01; ***, P < 0.001. Right: Single-cell expression of (left to right) pS6^{S235/236} or pAKT^{S473} (log₂ values). Red bar = geometric mean ± SD unpaired t test, two tails. *, P < 0.05; ***, P < 0.001. **(B)** Expression of (left to right) pAKT^{T308} (PI3K), pS6^{S235/236} (mTORC1), pAKT^{S473} (mTORC2), mTOR protein, and Bcl2 protein in the indicated NK cell subsets in adaptive NK cell-negative HDs. Violin plots, paired t test, parametric. *, P < 0.05; **, P < 0.01; ***, P < 0.001. **(C)** Schematic of the examined signaling and associated markers in the defined NK cells subsets.

mature adaptive NK cells, is associated with reduced mTOR activity (Fig. 3 C).

Peripheral blood FcRγ^{-/low} NK cells exhibit a differential FOXO1-EOMES-T-bet phenotype

mTORC2 suppresses the activity of the transcription factor FOXO1, a positive regulator of the transcription factor EOMES and a negative regulator of the transcription factor T-bet (Deng et al., 2015; Gordon et al., 2012). Both EOMES and T-bet regulate CD122 expression (Zhang et al., 2018). Therefore, we investigated FOXO1 activity in immature, mature nonadaptive, and adaptive NK cell subsets by examining T-bet, EOMES, and FOXO1 protein expression. T-bet levels were significantly lower in immature CD56^{bright}CD16⁻ and adaptive FcRγ^{low} or FcRγ⁻ NK cells relative to mature nonadaptive NK cells and similar to mTORC2 activity (Fig. 4 A). Accordingly, immature NK cells expressed higher EOMES and FOXO1 levels, explaining the

higher expression of CD122. However, adaptive NK cells expressed low EOMES and FOXO1 levels, explaining the decrease in CD122 expression (Fig. 4 A). In adaptive NK cell-negative HDs, T-bet levels increased with NK cell maturation, demonstrating a different expression pattern relative to adaptive NK cells (Fig. 4 B; Björkström et al., 2010). However, and in line with the reduced CD122 levels, EOMES and FOXO1 expression decreased with NK cell maturation, indicating that the reduction of these proteins is not specifically associated with the adaptive NK cell phenotype (Fig. 4 C). The results suggest a differential signaling regulation associated with alteration in mTORC2-FOXO1 activity and reduced FcRγ expression (Figs. 3 C and 4 C), whereas immature FcRγ^{low} NK cells are CD122^{high}, mTORC2^{low}, FOXO1^{high}, EOMES^{high}, and T-bet^{low}, and adaptive FcRγ^{low} or FcRγ⁻ NK cells are CD122^{low}, mTORC2^{low}, FOXO1^{low}, EOMES^{low}, and T-bet^{low}. Mature nonadaptive NKG2A⁻CD57⁺ NK cells, which are FcRγ^{high}, exhibited a CD122^{low}, mTORC2^{high}, FOXO1^{low}, EOMES^{low}, and

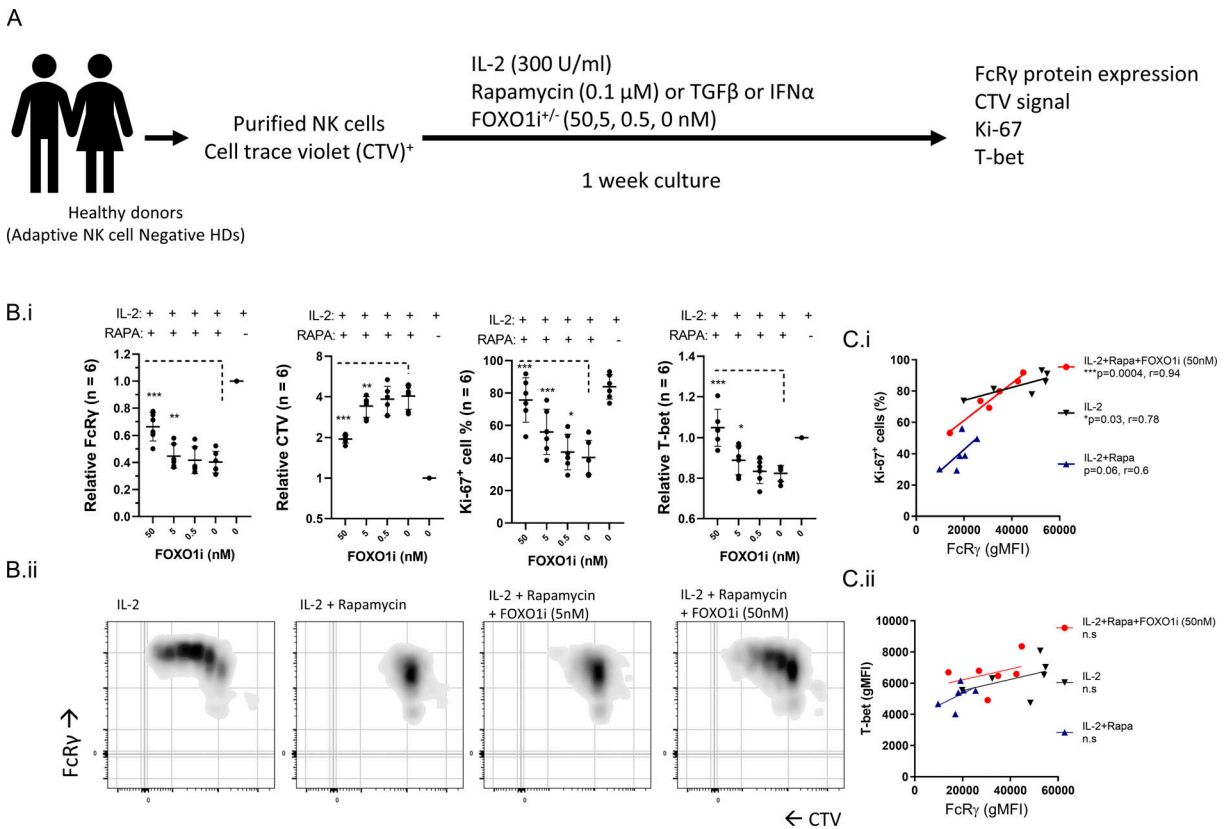


Figure 5. Cell proliferation control FcR γ upregulation. Purified primary NK cells from adaptive NK cell-negative HDs were stimulation as indicated and examined for the expression of the specified markers. Number of donors ($n = 6$), paired t test two tails or Pearson correlation, two tails. *, $P < 0.05$; **, $P < 0.01$; ***, $P < 0.001$. **(A)** Schematic of the experimental design. Purified NK cells were cultured in the presence of IL-2 (300 U/ml) and the mTOR inhibitor rapamycin (0.1 μ M; or TGF β or IFN α [Fig. 6]) and FOXO1 inhibitor at the indicated concentrations for 1 wk, and then examined for FcR γ upregulation, cell proliferation progression by CTV, induction of the proliferation marker Ki-67, and T-bet upregulation. Dead cells were gated out by viability dye. NK cells were gated as CD3-CD56 $^+$ cells. **(B i)** Analysis of (left to right) relative FcR γ expression, relative CTV values, percentages of Ki-67 $^+$ cells, and relative T-bet expression. Mean \pm SD, paired t -parametric. *, $P < 0.05$; **, $P < 0.01$; ***, $P < 0.001$. Values were normalized to culture with IL-2 alone to minimize variations between donors. **(B ii)** Representative density plot (with grid lines) of FcR γ expression vs. CTV values in the indicated conditions, showing increased FcR γ expression in proliferating cells. **(C)** Pearson correlation for each indicated condition between FcR γ vs. percentage of Ki-67 $^+$ cells (i) or FcR γ vs. T-bet expression (ii). One tail. *, $P < 0.05$; ***, $P < 0.001$.

IFN α induces STAT1 and STAT4 signaling, increases mTOR activity, and inhibits cell proliferation by elements such as IFN γ activation sites (Platanias, 2005). Therefore, we examined how TGF β or IFN α influences FcR γ expression in nonadaptive mature NK cells during IL-2 stimulation and cell proliferation (Fig. S3 C). Further, we examined the contribution of FOXO1 inhibition during TGF β or IFN α treatment. Increased TGF β or IFN α concentrations suppressed FcR γ upregulation relative to IL-2 stimulation alone (Fig. 6 A). IFN α stimulation increased mTOR activity, indicating that mTOR activation alone is insufficient to upregulate FcR γ expression (Fig. S3, C and D). As expected, TGF β or IFN α suppressed NK cell proliferation induced by IL-2 (Fig. 6, B and C). FcR γ upregulation significantly correlated with CTV dilution or increased percentage of Ki-67 $^+$ cells during TGF β or IFN α treatment (Fig. 6, D and E). In contrast and in line with mTOR activity, T-bet levels were suppressed by TGF β and increased by IFN α (Fig. 6 F). FOXO1i had a positive influence on FcR γ upregulation and on cell proliferation in cultures with low TGF β or IFN α concentrations (Fig. 6, A-C), suggesting the involvement of mechanisms suppressing FcR γ expression and cell

proliferation other than FOXO1 (Calnan and Brunet, 2008; Viel et al., 2016; Platanias, 2005). We concluded that FcR γ upregulation is dependent on cell proliferation downstream of various signaling pathways.

NK cells with an adaptive like-phenotype increase in the presence of IFN α and TGF β during COVID-19 infection

Adaptive NK cell numbers increase with COVID-19 disease severity and correlate with a poor outcome (Maucourant et al., 2020; Varchetta et al., 2021). Both IFN α and TGF β levels increase during COVID-19 infection and are associated with NK cell dysfunction (Krämer et al., 2021; Witkowski et al., 2021). Our analysis of NK cell subsets by protein and mRNA expression from a cohort of 139 COVID-19 patients with all levels of disease severity (defined by the World Health Organization Ordinal Scale [WOS] score: healthy donors = 0, mild = 1-2, moderate = 3-4, severe = 5-7; Su et al., 2020), at two different time points (T1 = baseline; Fig. 7, T2 = acute; Fig. S4; Su et al., 2020), indicated that the NK cell population changes with disease severity towards mature nonproliferative NK cells (Fig. 7 A and Fig. S4

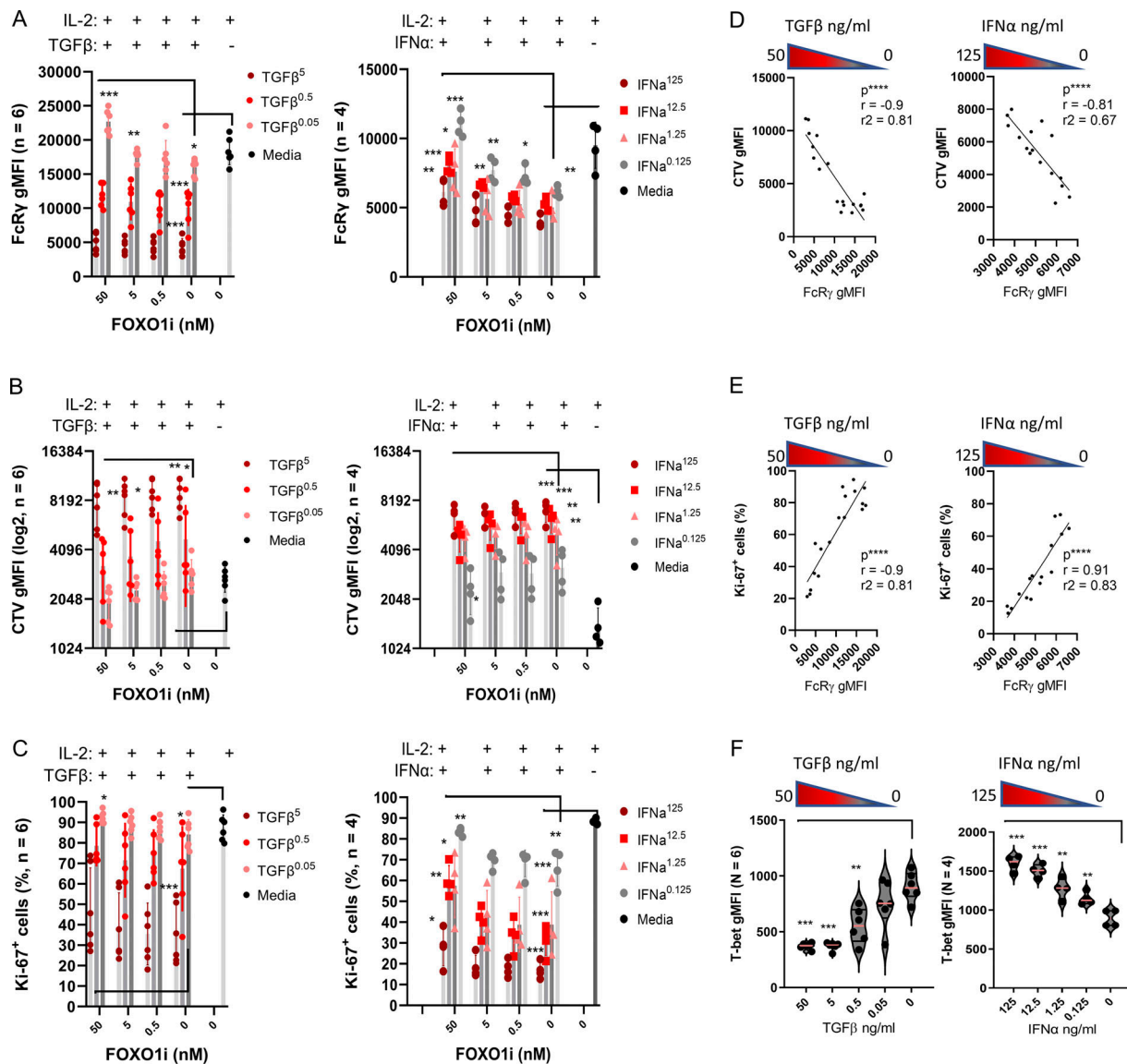


Figure 6. TGFβ or IFNα suppress FcRγ upregulation with correlation to cell proliferation. Purified primary NK cells from adaptive NK cell-negative HDs were stimulated as indicated (Fig. 5 A). Cultures with TGFβ (5, 0.5, 0.05 ng/ml) or IFNα (125, 12.5, 1.25, 0.125 ng/ml) in the presence of IL-2 (300 U/ml) ± FOXO1 inhibitor were performed as independent experiments. *n* = number of donors. Analysis of FcRγ expression, CTV dilution, or Ki-67 induction, is displayed relative to TGFβ (left) or IFNα (right) concentrations. Mean ± SD, paired *t* test, parametric. *, *P* < 0.05; **, *P* < 0.01; ***, *P* < 0.001. **(A)** FcRγ expression, gMFI levels. **(B)** CTV gMFI levels (log₂). **(C)** Percentage of Ki-67⁺ NK cells. **(D)** Pearson correlation between FcRγ vs. CTV gMFI levels. IL-2 cultures without FOXO1 inhibitor. Two tails, ***, *P* < 0.0001. **(E)** Pearson correlation between FcRγ vs. percentage of Ki-67⁺ NK cells. IL-2 cultures without FOXO1 inhibitor. Two tails, ***, *P* < 0.0001. **(F)** T-bet expression levels as an indicator of mTOR activity during IL-2 stimulation in the presence of the indicated TGFβ (left) or IFNα (right) concentrations. Two tails, ***, *P* < 0.0001.

A). Further, an IFNα gene signature (Krämer et al., 2021) and TGFβ or IL-15Rα plasma levels increased with disease severity and corresponded with lower NK cell percentages in peripheral blood and a reduction in the FcRγ gene expression in the NK cell population (Fig. 7 B and Fig. S4 B). Note that in the most severe disease, no significant change was seen in FcRγ gene expression compared to healthy donors, which might result from patients' death (Maucourant et al., 2020; Varchetta et al., 2021). Additionally, other adaptive NK cell-associated markers (e.g., PLZF (ZBTB16), Siglec-7 (SIGLEC7), CD161 (KLRB1), NKp30 (NCR3), NKp46 (NCR1), and Syk (SYK) exhibited reduced gene expression, while maturation markers (GZMB, BCL11B) increased, and

immature markers (GZMK) decreased, with no significant changes in CD3ζ (CD247) gene expression (Fig. 7 C and Fig. S4 D). Changes in gene patterns associated with an adaptive NK cell phenotype were significantly observed during the transition from mild to moderate disease severity (Fig. 7 C and Fig. S4 D), indicating a prognostic value for this early disease transition (Maucourant et al., 2020). The results show that the increase in NK cells with an adaptive-like phenotype during COVID-19 infection accrues in parallel to increased levels of IFNα, TGFβ, and IL-15Rα. This implies that higher TGFβ or IFNα levels might suppress IL-15-mediated cell proliferation and FcRγ upregulation, similar to their influence on IL-2.

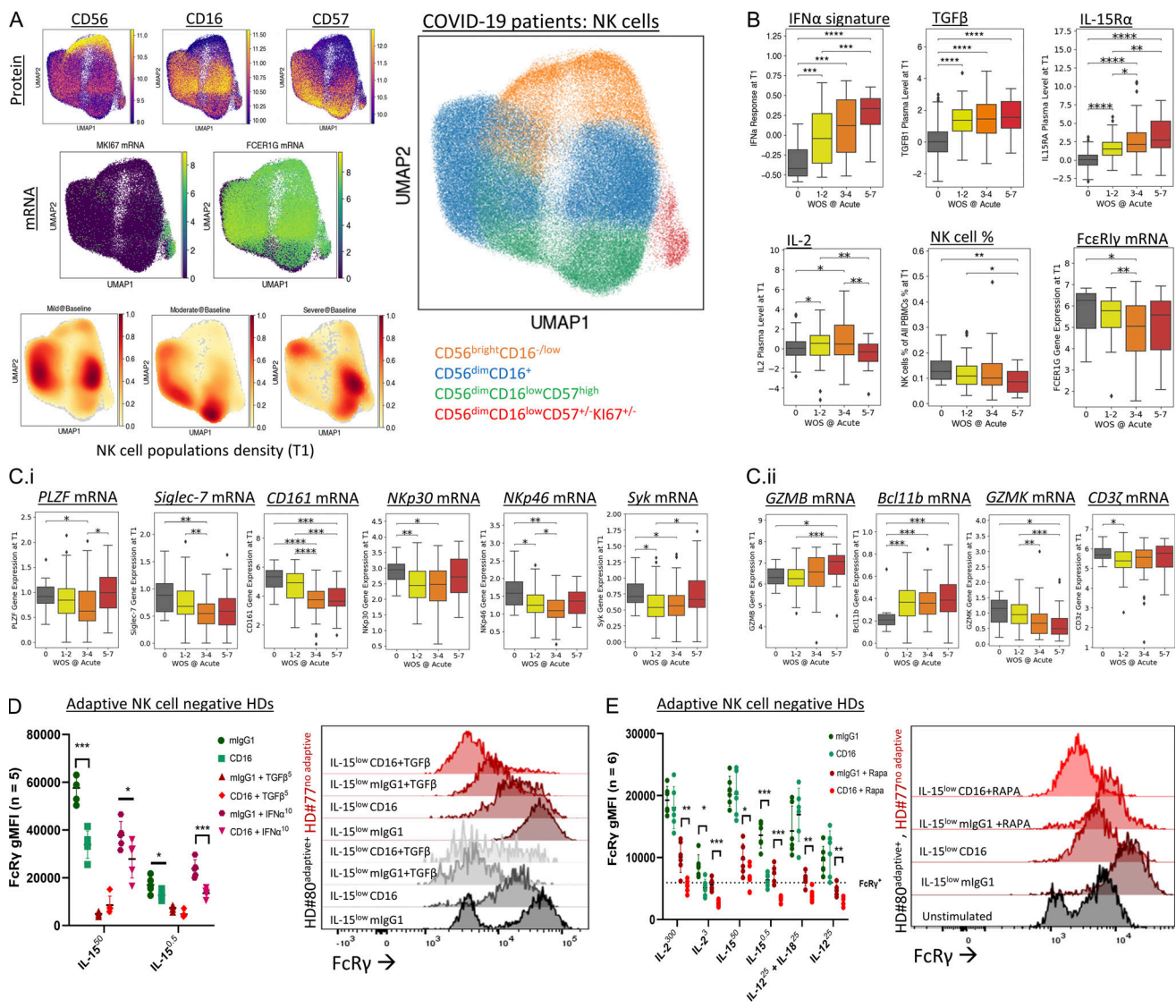


Figure 7. Increased IFN α gene signature and TGF β plasma levels during COVID-19 is associated with increased adaptive NK cell signature. (A) Characterization of NK cell subsets in a COVID-19 cohort. UMAP embedding of all NK cells colored by unsupervised clustering (top right) and by selected surface proteins (CD56, CD16, CD57 on top left three panels) and mRNA transcript levels of Ki-67 and Fc ϵ R γ . (B) Upper panels (left to right): IFN α response transcriptomic signature score in NK cells, TGF β levels in plasma, and IL-15R α plasma levels (as an indicator of IL-15 plasma levels). Lower panels (left to right): IL-2 plasma levels, NK cell percentages in PBMC, and Fc ϵ R γ gene expression in NK cells across patients with different WOS COVID-19 disease severity scores at baseline stage (T1). (C) Adaptive NK cell-associated gene expression for the markers (left to right: PLZF, Siglec-7, CD161, NKp30, NKp46, Syk; i) and maturation-associated markers (left to right: GZMB, Bcl11b, GZMK) and CD3 ζ (ii), within the NK cell population across patients with different WOS COVID-19 disease severity score at baseline stage (T1). (D) Fc ϵ R γ levels in NK cells, purified from adaptive NK cell-negative HDs, following 5 days IL-15 culture (ng/ml) with anti-CD16-coated beads relative to mouse IgG1 isotype-matched control-coated beads, with or without IFN α (10 ng/ml) or TGF β (5 ng/ml). Right: Representative histogram for Fc ϵ R γ expression in adaptive NK cell-negative HD (HD #77, red) relative to a control stimulated adaptive NK cell-positive HD (HD #80, black). (E) Fc ϵ R γ levels in NK cells, purified from adaptive NK cell-negative HDs, after 5 days of IL-2, IL-15, or IL-12 \pm IL-18 culture with anti-CD16-coated beads relative to mouse IgG1 isotype-matched control-coated beads, with or without rapamycin (0.1 μ M). Right: Representative histogram for Fc ϵ R γ expression in adaptive NK cell-negative HD (HD #77, red) relative to a control stimulated adaptive NK cell-positive HD (HD #80, black). COVID-19 analysis: Mann Whitney U test, *, P < 0.05; **, P < 0.01; ***, P < 0.001; ****, P < 0.0001. Ex vivo experiments: n = number of healthy donors, mean \pm SD, paired t test, two tails. *, P < 0.05; **, P < 0.01; ***, P < 0.001.

COVID-19 infection leads to an antibody-mediated response (Yu et al., 2021). CD16 stimulation has been reported to mediate adaptive Fc ϵ R γ ^{-low} NK cell expansion ex vivo and in vivo (Schlums et al., 2015; Lee et al., 2015). To examine the influence of CD16 stimulation and cell proliferation on Fc ϵ R γ levels, we stimulated purified NK cells from adaptive NK cell-negative HDs with agonist mouse anti-human CD16 antibody (IgG1)-coated

beads or with isotype-matched control mouse IgG1-coated beads. NK cells were cultured in the presence of increasing IL-15 concentrations with or without TGF β or IFN α . One adaptive NK cell-positive HD (#80, Fig. S2 A) was used as a control. CD16 stimulation in the presence of TGF β or IFN α significantly reduced Fc ϵ R γ protein expression, which was upregulated by IL-15 (Fig. 7 D). Stimulation of NK cells from an adaptive NK cell-

positive donor (black) with anti-CD16 and low concentrations of IL-15 led to an increase of FcR γ -positive cells (Fig. 7 D), whereas TGF β treatment led to an increase in adaptive NK cells. A similar observation was seen in NK cells from adaptive NK cell-negative HDs (red, Fig. 7 D). Additionally, CD16 stimulation (in the absence of TGF β or IFN α) of adaptive FcR γ ^{-low} NK cells relative to nonadaptive NK cells, sorted for CD57 expression, indicated a reduced cell proliferation capacity of adaptive NK cells in response to CD16 and IL-2 stimulation (Fig. S5 A), which aligned with reduced mTOR activation. Moreover, NKG2C stimulation did not increase the percentage of FcR γ -negative cells (Fig. S5 B). mTOR inhibition, during CD16 stimulation and IL-2, IL-15, or IL-12 \pm IL-18, led to a significant reduction in FcR γ protein expression in NK cells from adaptive NK cell-negative HDs and relative to an unstimulated adaptive NK cell-positive donor control (black, Fig. 7 E). Thus, CD16 stimulation synergizes with cell proliferation suppression to facilitate the acquisition of an NK cell FcR γ ^{-low} adaptive-like phenotype.

Discussion

In this study, we discovered reduced FcR γ protein expression in peripheral blood NK cell subsets from human lung transplant patients undergoing treatment with rapamycin. Further, we observed that in healthy individuals, peripheral blood immature and mature adaptive NK cells, which express lower FcR γ levels, display reduced mTOR activity. We further showed that cell proliferation during IL-2 receptor stimulation is involved in FcR γ protein regulation. Thus, the strength of IL-2 receptor stimulation, the level of mTOR activity, or/and modulation of FOXO1 activity that influence cell proliferation are all essential for the regulation of FcR γ protein expression (Wang and Zhao, 2021). We further showed that TGF β or IFN α stimulation suppressed FcR γ upregulation independently of mTOR or FOXO1 activity (Viel et al., 2016; Platanius, 2005). This shows that besides mTOR activation and FOXO1 suppression, other signaling pathways, such as Smad signaling (Viel et al., 2016) or STAT1 signaling (Platanius, 2005), which are reported to inhibit NK cell proliferation, suppress FcR γ expression (Liu et al., 2020; Krämer et al., 2021; Witkowski et al., 2021; Shemesh et al., 2022). In line with these results, we showed that the increase in mature NK cells with an adaptive-like phenotype during COVID-19 infection is associated with increased TGF β and IFN α levels and increased disease severity. Further, suppressing NK cell proliferation during CD16 stimulation diminished FcR γ protein expression and increased the acquisition of the FcR γ ^{-low} phenotype reported in adaptive NK cells (Pahl et al., 2018).

In healthy donors, mature adaptive NK cells and immature NK cells displayed reduced mTOR activity. Additionally, adaptive NK cells have reduced CD122 surface levels and low FOXO1 expression. Consequently, in adaptive NK cells, limited IL-2 receptor signaling, mediated by lower CD122 expression and reduced mTOR activity (Marçais et al., 2014), would lead to diminished NK cell proliferation and lower FcR γ expression in this NK cell subset. Similarly, pSTAT4 and pSTAT5, which were reported to induce genes necessary for NK cell proliferation and are antagonized by Smad, STAT1, or FOXO1, were decreased in

adaptive NK cells and (Wang and Zhao, 2021; Calnan and Brunet, 2008; Ouyang and Li, 2011). This suggests the contribution of STAT4 and STAT5 in FcR γ upregulation are parallel to and under the regulation of mTOR activity. In the context of IFN α or TGF β signaling, pSTAT1 levels decrease with the adaptive phenotype but we could not detect evidence for Smad signaling in adaptive NK cells from HDs (our unpublished data). Thus, the contribution of IFN α or TGF β to the adaptive NK cell phenotype in healthy donors is unclear. This might suggest an early differentiation event associated with a chronic or severe viral infection, as seen during COVID-19. However, we cannot exclude the contribution of undiscovered mechanisms that suppress mTOR activity in adaptive NK cells. These observations demonstrate that the FcR γ ^{-low} phenotype is regulated by various signaling pathways associated with diminished cell proliferation.

Our results indicate that the *in vivo* expansion of adaptive or adaptive-like NK cells is not mediated by a higher cell proliferation rate as we have shown that proliferation results in the upregulation, not down regulation, of FcR γ expression. However, accumulation of adaptive or adaptive-like NK cells might result from slow homeostatic proliferation mediated by continuous activating receptor stimulation of these NK cells (Sun et al., 2011; Steinbach et al., 2018). In humans, tissue-resident NK cells display an adaptive-like phenotype (Brownlie et al., 2021). One can speculate that tissue residency might promote diminished NK cell proliferation to increase persistence and generate tissue-specific adaptive-like NK cells with enhanced CD16-mediated functions by inhibiting FcR γ expression (Liu et al., 2020). In contrast to humans, the accumulation of FcR γ ^{-low} NK cells does not occur during murine cytomegalovirus (MCMV) infection and the expansion of adaptive mouse NK cells, while several reports show their existence and CMV-related expansion in Rhesus macaques (Shah et al., 2018). This discrepancy might be due to several reasons. Maturation of the immune system is related to diverse microbial exposure (Tao and Reese, 2017), which differs in humans and laboratory-housed inbred mice. Variation in cytokine sensitivity between species might allow the survival of human adaptive FcR γ ^{-low} NK cells (Lebrec et al., 2013). Alternatively, the absence of FcR γ ^{-low} NK cells in mice may be due to differences in the MCMV model and HCMV infection (Sun et al., 2009) or differences in mouse NK cell activating receptor expression. For example, due to the lack of CD3 ζ signaling induced by CD16 in mouse NK cells (Shah et al., 2018; Aguilar et al., 2022), the absence of NKp30 and NKG2C expression in mice (Hollyoake et al., 2005; Lanier et al., 1998), or the requirement of CD3 ζ signaling for receptor-mediated adaptive NK cell expansion or persistence in humans (Sun et al., 2011; Shah et al., 2018).

Overall, our results suggest that the mechanism regulating the expansion of mature adaptive or adaptive-like FcR γ ^{-low} human NK cells differs from mouse Ly49H⁺ NK cell or human NKG2C⁺ NK cell expansion during early CMV infection (Cerwenka and Lanier, 2016). Our observations align with a reduced NK cell proliferation associated with NK cell maturation (Cooper et al., 2001), with biochemical analysis reporting FCER1 promoter demethylation or regulation by cell cycle-related

proteins (Correia et al., 2018; Takahashi et al., 2008; Tapias et al., 2008), and with mouse NK cell expansion during MCMV infection associated with increased PLZF levels and reduced Bcl2 levels (Beaulieu et al., 2014; Viant et al., 2017).

One potential explanation for differences in mTOR activity in NK cell subsets is the interplay between tonic signaling of activating or inhibitory receptors or the accumulation of putative “exhaustion” markers (e.g., TIM3 or LAG3; Myers et al., 2019; Anton et al., 2015; Holmes et al., 2021). In CD8⁺ T cells, tonic TCR-MHC signaling regulates cytokine sensitivity (Cho et al., 2010), which is reported to decrease in adaptive NK cells (Liu et al., 2020), while PD-1 or inhibitory receptors can suppress mTOR activity (Staron et al., 2014; Goodridge et al., 2019; Jia and Bonifacino, 2019). However, overstimulation of activating receptors can also reduce mTOR activity in NK cells (Marçais et al., 2017). In the context of FcγR expression, FcγR knockout leading to low NKp30 and NKp46 surface expression does not alter human NK cell proliferation (Ki-67 expression) or cytokine sensitivity, suggesting these changes are upstream of or parallel to FcγR expression (Liu et al., 2020).

Reduced mTORC2 activity is associated with memory T cell differentiation through increased FOXO1 activity and maintaining EOMES and CD122 expression (Zhang et al., 2016), similar to immature NK cells. Short-lived effector CD8⁺ T cells are characterized as mTOR^{high}FOXO1^{low}T-bet^{high}, similar to mature nonadaptive NK cells. FOXO1 activity suppresses T-bet to promote memory CD8⁺ T cells differentiation and maintenance during chronic viral infections to prevent anergy (Rao et al., 2012; Delpoux et al., 2018). Therefore, loss of FOXO1 expression with low mTOR activity might be associated with NK cell anergy (Ardolino et al., 2014; Zhang et al., 2018). In our analysis, peripheral blood adaptive NK cells were CD122^{low}mTORC1/C2^{low} FOXO1^{low}EOMES^{low}T-bet^{low}; therefore, showing an NK cell “adaptive” signaling phenotype resembling effector-memory, exhausted, and senescence CD8⁺ T cells, distinct from NK cell maturation associated with increased effector functions (Lopez-Vergès et al., 2010). Interestingly, an NK1.1⁻NKp46⁻EOMES^{low}T-bet^{low} phenotype is reported for mouse NK cell progenitors, which require IL-15- or IL-12-mediated signaling to develop a mature NK cell phenotype and effector functions (Zhang et al., 2018; Ohs et al., 2016). Thus, human adaptive NK cell differentiation, reported to exhibit reduced cytokine sensitivity (Liu et al., 2020), might indicate a reversion to a progenitor-like signaling phenotype and might be less dependent on IL-2 or IL-15 signaling for long-term survival (Sun et al., 2011).

Low mTOR activity and T-bet expression dampen NK cell responses against tumors and are associated with NK cell hyporeactivity (Gordon et al., 2012; Michelet et al., 2018; Mao et al., 2016; Daher et al., 2021). Yet, adaptive NK cells show positive antitumor responses dependent on HLA-E expression on tumors and an individuals’ HCMV serostatus (Merino et al., 2021; Anton et al., 2015). In contrast, single-cell profiling of adaptive NK cells suggests impaired functions (Zaghi et al., 2021). Others have reported diminished NK cell functions associated with increased IFNα or TGFβ levels during COVID-19 (Krämer et al., 2021; Witkowski et al., 2021). Thus, the increased ex vivo activity

associated with adaptive NK cells might be model specific and dependent on ligand expression and cytokines in the microenvironment. Reduced NKp30 or NKp46 expression, regulated by FcγR, is a poor prognosis marker in acute myeloid leukemia, is associated with damped NK cell functions against several cancer types, and might explain the low NK cell activity observed in COVID-19 patients (Chretien et al., 2017b; Chretien et al., 2017a; Romee et al., 2016; Zhuang et al., 2019; Walk and Sauerwein, 2019). We and others have shown that the increase in NK cells with an adaptive-like phenotype during COVID-19 infection accrues with a decrease in total NK cells, which might limit NK cell antibody-mediated responses in vivo (Lanier et al., 1991; Yu et al., 2021). According to our data, the increase in the adaptive-like NK cell phenotype during COVID-19 infection might also reflect an early prognostic marker and suggest blocking TGFβ as a therapeutic strategy (Witkowski et al., 2021). Our observations also suggest that mTORC2 inhibition by specific antagonists might improve in vivo NK cell functions mediated by CD16 (Rozenfurt et al., 2014). In conclusion, our findings indicate that the adaptive or adaptive-like FcγR^{-/low} NK cell phenotype is regulated by multiple signaling pathways associated with diminishing NK cell proliferation and provide a strategy to therapeutically manipulate adaptive or adaptive-like NK cell immunity in COVID-19 infection.

Materials and methods

Lung transplant recipients’ samples

The University of California, San Francisco (UCSF) Institutional Review Board (#13-10738; IRB) approved this study. PBMCs were isolated from patients’ peripheral blood after they gave informed consent. Lung transplant recipient standard maintenance immunosuppressant therapy included tacrolimus, prednisone, and mycophenolate mofetil. Tacrolimus troughs of 8–14 ng/ml were targeted during the first 12 mo after transplant and 6–10 ng/ml after that. All subjects were started on 20 mg of prednisone daily and reduced to a goal dose of 0.1 mg/kg over the first postoperative year. Sirolimus (rapamycin) is used as adjunctive therapy as a treatment for chronic lung allograft dysfunction or recurrent episodes of acute cellular rejection. In addition, sirolimus is prescribed as a calcineurin-inhibitor sparing agent when recipients develop chronic kidney disease or recurrent skin carcinomas. PBMCs were prospectively collected and cryopreserved from lung transplant recipients during routine clinic visits. Four subjects were identified with PBMCs available before and during therapeutic sirolimus treatment, which was targeted through blood drug levels. PBMCs were available from five control lung transplant subjects that were at least 1-yr post-transplant and matched for transplant indication.

Primary NK cells isolation

Primary human NK cells were obtained from healthy donors’ peripheral blood after donors gave informed consent in accordance with approval by the UCSF IRB (#10-00265) or from Plateletpheresis leukoreduction filters (Vitalant, <https://vitalant.org/Home.aspx>). NK cell isolation was done by using the negative selection “RosetteSep Human NK Cell Enrichment

Cocktail” kit (#15065; STEMCELL Technologies) according to the company’s protocol. Adaptive NK cell-positive or -negative healthy donors were identified by staining purified ex vivo unstimulated NK cells for live (near infra-red-fixable dye-negative cells) CD3⁻ cells expressing surface CD56, CD16, CD57, NKG2C, and NKG2A and intracellular FcRγ.

Flow cytometry

Ex vivo NK cells (5×10^4 cells/well) or NK cells following the specified stimulation were collected, and culture media was washed out using flow buffer (PBS with 2% FCS). For surface membrane staining, antibodies were resuspended in PBS + 2% FCS and incubated with the cells for 30 min at 4°C at 50 μl/well. Dead cells were excluded by labeling using Zombie-red (1:1,000, #77475; BioLegend) or near-infra-red-fixable dye (1:1,000, #L34976; Invitrogen). Antibodies were washed out by adding 150 μl/well of flow buffer. Following centrifugation at 600 g rcf for 5 min at 4°C, flow buffer was discarded. For surface staining, samples were suspended in 300 μl flow buffer and kept on ice until the sample was processed. For intracellular protein expression, cells were incubated for 20 min at 4°C with 100 μl/well Cytofix/Cytoperm buffer (#51-2090KZ; Becton Dickinson). Following incubation, cells were washed twice using 150 μl/well intracellular-staining Perm-Wash buffer (#421002; BioLegend) diluted 1:10 in PBS, and centrifugation at 600 g rcf for 5 min at 4°. Perm-Wash buffer was discarded after centrifugation. Antibodies against intracellular markers were diluted in Perm-Wash buffer and incubated with the cells for 60 min at 4°C. Following incubation, cells were washed twice with 150 μl/well Perm-Wash buffer. Before analyzing the samples for surface or/and intracellular markers, cells were resuspended in a 300 μl flow buffer. Samples were kept at 4°C until the sample was processed. Data acquisition was performed using an LSR-II flow cytometer and analysis was performed by using FlowJo.v10.

Flow cytometry analysis of lung transplant patients

Lymphocytes in the PBMCs were gated as CD45⁺ (#304024; BioLegend), live cells (Zombie red-negative, #77475; BioLegend), and singlet cells based on forward-angle light-scattering properties (forward scatter area vs. forward scatter height). Non-NK cells were excluded by staining with anti-CD3 (#300318, RRI-D:AB_314054; BioLegend), -CD19 (#302218, RRID:AB_314248; BioLegend), -CD4 (#357416, RRID:AB_2616810; BioLegend), -CD14 (#301820, RRID:AB_493695; BioLegend), and -CD123 (#306042, RRID:AB_2750163; BioLegend). NKp46⁺ cells were gated as NKG2A vs. CD16. NKG2A-negative CD16-negative cells were excluded as they could not be defined as a specific NK cell subset. Antibodies used to define NK cell subsets: anti-CD56 (#318322, RRID:AB_893389; BioLegend), -NKp46 (#331936, RRID:AB_2650940; BioLegend), -CD16 (#302038, RRID:AB_2561578; BioLegend), and -NKG2A (#130-113-567, RRID:AB_2726172). Human Fc receptors were blocked using human TruStain FcXTM (#422302, RRID:AB_2818986; BioLegend).

Ex vivo unstimulated human primary NK cells signaling molecules analysis

Freshly isolated, unstimulated human primary NK cells were intracellularly stained for STATs phosphorylation (pSTAT1^{Y701},

pSTAT4^{Y963}, pSTAT5^{Y964}), PI3K activity (pAKT^{T308}), mTORC1 activity (pS6^{S235/236}), mTORC2 activity (pAKT^{S473}), mTOR, Bcl2, T-bet, EOMES, or FOXO1 protein expression. Data from adaptive NK cell-positive HDs were collected on the date of cell isolation and normalized to minimize variations between donors due to different isolation dates caused by the rarity of adaptive NK cell-positive HDs (<10% of the human population). Data normalization was performed by dividing the geometric mean fluorescence intensity (gMFI) of each defined NK cell population relative to live (near-infra-red-fixable dye negative cells) mature CD3⁻CD56^{dim}CD16⁺CD57⁻NKG2C⁻FcRγ^{high} NK cells (index = 1). Data normalization was additionally performed for adaptive NK cell makers: PLZF, Syk, NKp30, NKp46, CD161, Siglec-7, and ADAM10 or CD132. Adaptive NK cell-negative HDs data acquisition was performed on the same date and therefore was not normalized.

NK cell stimulation and cell division assays

Ex vivo unstimulated NK cells were labeled with CTV dye according to the company’s protocol (#C34557; Invitrogen). The assay was performed in 96-well round-bottom plates. Antibody-coated beads were diluted 1:500 from stock (0.1 μg antibody/μl) in cytokine-free NK cell culture media and used at 50 μl/well. IL-2, IL-15, IL-12, IL-18, TGFβ, IFNα, FOXO1i, or rapamycin were prepared at ×4 concentration and used at 50 μl/well. Accordingly, 50–100 μl/well of cytokine-free NK cell culture media were supplemented to reach a culture media volume of 150 μl/well. At the final step, CTV-labeled NK cells were added at 5×10^4 cells/well, 50 μl/well, to reach a final volume of 200 μl/well. NK cells were incubated at 37°C with 5% CO₂ for the assay duration. CTV signal was analyzed by flow cytometry (LSR-II; Becton Dickinson Immunocytometry Systems). For cell division assays without activating receptor stimulation, the CTV signal was analyzed on day 6, while with activating receptor stimulation on day 5 due to variation in cell proliferation rate. Dead cells were gated out by near-infra-red-fixable dye (1:1,000, #L34976; Invitrogen). NK cell culture media was Good Manufacturing Practices grade Stem Cell Growth Medium (CellGenix) supplemented with 1% L-glutamine, 1% penicillin and streptomycin, 1% sodium pyruvate, 1% nonessential amino acids, 10 mM Hepes, and 10% human serum (heat-inactivated, sterile-filtered, male AB plasma; Sigma-Aldrich).

COVID-19 patient samples

Longitudinal blood samples from 139 COVID-19 patients (60 males and 79 females; 265 samples from 2 longitudinal blood draws per patient) were analyzed through single-cell RNA sequencing (scRNA-seq) and CITE-seq analysis and plasma proteomics (Providence St. Joseph Health with IRB Study Number STUDY2020000175 and the Western Institutional Review Board with IRB Study Number 20170658), as was previously described (Su et al., 2020). All blood scRNA-seq data used in this study can be found under the ArrayExpress accession number E-MTAB-9357. One blood draw was collected shortly after the initial clinical diagnosis (time = T1, diagnosis stage), and the second blood draw was collected a few days later (T2, acute stage). The severity of COVID-19 disease clinical status was assessed

throughout a patient's encounter in accordance with the nine-point WOS and further classified into mild (WOS = 1-2); moderate (WOS = 3-4), and severe (WOS = 5-7) groups.

Antibody-conjugated beads

Antibody-conjugated beads were prepared according to the company's protocol (Invitrogen Dynabeads Antibody Coupling Kit) at 10 µg antibody for 1-mg beads. Following conjugation, beads were resuspended in sterile PBS at an antibody concentration of 0.1 µg/µl. Antibody conjugation was evaluated by flow cytometry with APC-conjugated anti-mouse or -rat IgG. Anti-human CD16 (#302002, mouse IgG1k; BioLegend) and mouse IgG1 isotype matched-control (UCSF Monoclonal Antibody Core, clone MOPC-21) were used. Antibody-conjugated beads were stored at 4°C.

Cytokines and inhibitors

All cytokines were resuspended in sterile PBS: human IL-2, 1,000 U/µl (TECINTM; teceleukin, ROCHE, generously provided by NCI Biological Resources Branch); human IL-15, 250 µg/ml (#247-IL/CF; R&D Systems); human TGFβ1, 50 µg/ml (#580706; BioLegend); human IFN α 2A (#78076; STEMCELL); human IL-12, 50 µg/ml (#219-IL; R&D Systems); and human IL-18, 50 µg/ml (#9124-IL/CF; R&D Systems). mTORC1 inhibitor (Calbiochem; rapamycin, #553210, IC₅₀ = 0.1 µM), and FOXO1 inhibitor Calbiochem (AS1842856, #344355, IC₅₀ = 33 nM) were suspended in DMSO. Cytokines or inhibitors were stored at -20°C.

Antibodies

The following antibodies were used: BioLegend: APC-Cy7-conjugated anti-CD3 (#300318, RRID:AB_314054), PerCep-Cy5.5 anti-CD56 (#318322, RRID:AB_893389), APC-conjugated anti-CD16 (#02012, RRID:AB_314212), or BV-421-conjugated anti-CD16 (#302038, RRID:AB_2561578) or PE-Cy7-conjugated anti-CD16 (#360708, RRID:AB_2562951), and BV605-conjugated anti-CD57 (#393304, RRID:AB_2728426) or APC-conjugated anti-CD57 (#322314, RRID:AB_2063199). R&D Systems: PE- or APC-conjugated anti-NKG2C (#FAB138P, RRID:AB_2132983 or #FAB138A, RRID:AB_416838—generously provided by R&D Systems). NK cells were then stained for intracellular expression with FITC-conjugated anti-FcRγ (#FCABS400F, RRID:AB_11203492; Millipore). For detection of surface or intracellular proteins: BioLegend: APC-conjugated anti-NKp30 (#325210, RRID:AB_2149449), APC-conjugated anti-NKp46 (#331918, RRID:AB_2561650), APC-conjugated anti-Siglec-7 (#339206), APC-conjugated anti-CD161 (#339912), APC-conjugated anti-CD25 (#302610, RRID:AB_314280), APC-conjugated anti-CD122 (#339008, RRID:AB_2123575), PE-conjugated anti-CD132 (#338605, RRID:AB_1279079), APC-conjugated anti-SYK (#644305, RRID:AB_2687145), APC-conjugated anti-T-bet (#644813, RRID:AB_10896913), and APC-conjugated anti-ADAM10 (#352705, RRID:AB_2563172). R&D Systems: AF647-conjugated anti-PLZF (#IC2944R) and AF647-conjugated anti-EOMES (#IC6166R). Becton Dickinson: APC-conjugated anti-CD122 (Mik-β3, #566620, RRID:AB_2869796), AF647-conjugated anti-pSTAT4-Y693 (#562074, RRID:AB_10896660), AF647-conjugated anti-pSTAT5-Y694 (#612599, RRID:AB_399882), AF647-conjugated anti-pSTAT1-Y701 (#612597, RRID:AB_399880), AF647-conjugated anti-Bcl-2 (#563600,

RRID:AB_2738306), AF647-conjugated anti-Ki-67 (#558615, RRID:AB_647130). Cell Signaling: AF647-conjugated anti-pS6-S235/236 (#4851, RRID:AB_10695457), AF647-conjugated anti-pAKT-T308 (#48646, RRID:AB_2799341), AF647-conjugated anti-pAKT-S473 (#4075, RRID:AB_916029), AF647-conjugated anti-mTOR (#5048, RRID:AB_10828101), and AF647-conjugated anti-FOXO1 (#72874, RRID:AB_2799829). Miltenyi-Biotech: APC-conjugated anti-NKG2A (#130-114-089, RRID:AB_2726447) and PE-vio-770-conjugated anti-NKG2A (#130-113-567, RRID:AB_2726172).

Graphics and statistical analysis

Graphs were generated using GraphPad Prism 5 or FlowJo_V10. Statistical analysis, as indicated in figure legends, was calculated using GraphPad Prism 9 or Excel (Microsoft 365). *, P ≤ 0.05; **, P < 0.01; ***, P < 0.001; ****, P < 0.0001. Statistical tests are described in figure legends. All experiments were performed as n ≥ 2 independent experiments.

Online supplemental material

Fig. S1 shows lung transplant patients' clinical information, and NK cell percentages and markers. **Fig. S2** shows healthy donors' NK cell gating strategy and donors' information. **Fig. S3** shows characterization of ex vivo primary adaptive NK cells. **Fig. S4** shows characterization of COVID-19 blood samples. **Fig. S5** shows influence of CD16 or NKG2C stimulation on adoptive FcRγ^{low} NK cells.

Acknowledgments

We are thankful to the organ and tissue donors, and their families for giving gifts of life and knowledge with their generous donation, and the UCSF Parnassus Flow Core (RRID:SCR_018206 and D.R. Calabrese Center Grant NIH P30 DK063720). We acknowledge Emily Aminian, Lily Tran, Jon Singer, Steve Hays, and the remainder of the lung transplant clinical team for instrumental aid in subject recruitment and sample processing.

Studies were supported by National Institutes of Health grant AI068129, the Parker Institute for Cancer Immunotherapy, and the Irvington Cancer Research Institute Fellowship to A. Shemesh, the Joel D. Cooper Award from the International Society for Heart and Lung Transplantation (D.R. Calabrese), the Cystic Fibrosis Foundation Harry Shwachman Career Development Award CALABR19Q0 (D.R. Calabrese), the Veterans Affairs Office of Research and Development (CX002011, J.R. Greenland) and National Heart, Lung, and Blood Institute (HL151552, J.R. Greenland).

Author contributions: Conceptualization: A. Shemesh and L.L. Lanier. Data curation: A. Shemesh, Y. Su, and D. Chen. Formal analysis: A. Shemesh, Y. Su, and D. Chen. Funding acquisition: L.L. Lanier, A. Shemesh, K.T. Roybal, D.R. Calabrese, J.R. Greenland, and J.R. Heath. Investigation: A. Shemesh, J. Arakawa-Hoyt, Y. Su, and D. Chen. Methodology: A. Shemesh, Y. Su, and D. Chen. Project administration: A. Shemesh and L.L. Lanier. Resources: D.R. Calabrese, J.R. Greenland, Y. Su, D. Chen, and J.R. Heath. Supervision and validation: A. Shemesh and L.L. Lanier. Visualization: A. Shemesh and D. Chen. Writing, original

draft: A. Shemesh and L.L. Lanier. Writing, review & editing: A. Shemesh, Y. Su, D.R. Calabrese, D. Chen, K.T. Roybal, J.R. Heath, J.R. Greenland, and L.L. Lanier. Supervision: L.L. Lanier.

Disclosures: K.T. Roybal reported personal fees from Arsenal Bio, Venrock, and Alaunos Therapeutics outside the submitted work; in addition, K.T. Roybal is a consultant, SAB member, and stockholder in Arsenal Biosciences, an SAB member at Alaunos Therapeutics, and an advisor for Venrock. J.R. Heath reported grants from Merck and Gilead and nonfinancial support from Isoplex during the conduct of the study; and personal fees from Regeneron and PACT Pharma outside the submitted work. J.R. Greenland reported personal fees from Theravance Biopharma outside the submitted work. No other disclosures were reported.

Submitted: 28 March 2022

Revised: 14 June 2022

Accepted: 5 August 2022

References

Aguilar, O.A., L.-K. Fong, K. Ishiyama, W.F. DeGrado, and L.L. Lanier. 2022. The CD3 ζ adaptor structure determines functional differences between human and mouse CD16 Fc receptor signaling. *J. Exp. Med.* 219: e20220022. <https://doi.org/10.1084/jem.20220022>

Anton, O.M., M.E. Peterson, M.J. Hollander, D.W. Dorward, G. Arora, J. Traba, S. Rajagopalan, E.L. Snapp, K.C. Garcia, T.A. Waldmann, and E.O. Long. 2020. Trans-endocytosis of intact IL-15R α -IL-15 complex from presenting cells into NK cells favors signaling for proliferation. *Proc. Natl. Acad. Sci. USA.* 117:522–531. <https://doi.org/10.1073/pnas.1911678117>

Anton, O.M., S. Vielkind, M.E. Peterson, Y. Tagaya, and E.O. Long. 2015. NK cell proliferation induced by IL-15 transpresentation is negatively regulated by inhibitory receptors. *J. Immunol.* 195:4810–4821. <https://doi.org/10.4049/jimmunol.1500414>

Ardolino, M., C.S. Azimi, A. Iannello, T.N. Trevino, L. Horan, L. Zhang, W. Deng, A.M. Ring, S. Fischer, K.C. Garcia, and D.H. Raulet. 2014. Cytokine therapy reverses NK cell anergy in MHC-deficient tumors. *J. Clin. Invest.* 124:4781–4794. <https://doi.org/10.1172/JCI74337>

Augustine, J.J., K.A. Bodziak, and D.E. Hricik. 2007. Use of sirolimus in solid organ transplantation. *Drugs.* 67:369–391. <https://doi.org/10.2165/00003495-200767030-00004>

Barnes, S., O. Schilizzi, K.M. Audsley, H.V. Newnes, and B. Foley. 2020. Deciphering the immunological phenomenon of adaptive natural killer (NK) cells and cytomegalovirus (CMV). *Int. J. Mol. Sci.* 21:8864. <https://doi.org/10.3390/ijms21228864>

Beaulieu, A.M., C.L. Zawislak, T. Nakayama, and J.C. Sun. 2014. The transcription factor Zbtb32 controls the proliferative burst of virus-specific natural killer cells responding to infection. *Nat. Immunol.* 15:546–553. <https://doi.org/10.1038/ni.2876>

Björkström, N.K., P. Riese, F. Heuts, S. Andersson, C. Fauriat, M.A. Ivarsson, A.T. Björklund, M. Flodström-Tullberg, J. Michaëlsson, M.E. Rottenberg, et al. 2010. Expression patterns of NKG2A, KIR, and CD57 define a process of CD56dim NK-cell differentiation uncoupled from NK-cell education. *Blood.* 116:3853–3864. <https://doi.org/10.1182/blood-2010-04-281675>

Brownlie, D., M. Scharenberg, J.E. Mold, J. Hård, E. Kekäläinen, M. Buggert, S. Nguyen, J.N. Wilson, M. Al-Ameri, H.-G. Ljunggren, et al. 2021. Expansions of adaptive-like NK cells with a tissue-resident phenotype in human lung and blood. *Proc. Natl. Acad. Sci. USA.* 118:e2016580118. <https://doi.org/10.1073/pnas.2016580118>

Calabrese, D.R., E. Aminian, B. Mallavia, F. Liu, S.J. Cleary, O.A. Aguilar, P. Wang, J.P. Singer, S.R. Hays, J.A. Golden, et al. 2021. Natural killer cells activated through NKG2D mediate lung ischemia-reperfusion injury. *J. Clin. Invest.* 131:e137047. <https://doi.org/10.1172/JCI137047>

Calnan, D.R., and A. Brunet. 2008. The FoxO code. *Oncogene.* 27:2276–2288. <https://doi.org/10.1038/ncr.2008.21>

Cerwenka, A., and L.L. Lanier. 2016. Natural killer cell memory in infection, inflammation and cancer. *Nat. Rev. Immunol.* 16:112–123. <https://doi.org/10.1038/nri.2015.9>

Cho, J.-H., H.-O. Kim, C.D. Surh, and J. Sprent. 2010. T cell receptor-dependent regulation of lipid rafts controls naive CD8⁺ T cell homeostasis. *Immunity.* 32:214–226. <https://doi.org/10.1016/j.immuni.2009.11.014>

Chretien, A.-S., R. Devillier, C. Fauriat, F. Orlanducci, S. Harbi, A. Le Roy, J. Rey, G. Bouvier Borg, E. Gautherot, J.-F. Hamel, et al. 2017a. NKP46 expression on NK cells as a prognostic and predictive biomarker for response to allo-SCT in patients with AML. *Oncotarget.* 6: e1307491. <https://doi.org/10.1080/2162402X.2017.1307491>

Chretien, A.-S., C. Fauriat, F. Orlanducci, J. Rey, G.B. Borg, E. Gautherot, S. Granjeaud, C. Demerle, J.-F. Hamel, A. Cerwenka, et al. 2017b. NKP30 expression is a prognostic immune biomarker for stratification of patients with intermediate-risk acute myeloid leukemia. *Oncotarget.* 8: 49548–49563. <https://doi.org/10.18632/oncotarget.17747>

Cooper, M.A., T.A. Fehniger, and M.A. Caligiuri. 2001. The biology of human natural killer-cell subsets. *Trends Immunol.* 22:633–640. [https://doi.org/10.1016/S1471-4906\(01\)02060-9](https://doi.org/10.1016/S1471-4906(01)02060-9)

Correa, M.P., A. Stojanovic, K. Bauer, D. Juraeva, L.-O. Tykocinski, H.-M. Lorenz, B. Brors, and A. Cerwenka. 2018. Distinct human circulating NKP30+Fc ϵ R1 γ +CD8⁺ T cell population exhibiting high natural killer-like antitumor potential. *Proc. Natl. Acad. Sci. USA.* 115:E5980–E5989. <https://doi.org/10.1073/pnas.1720564115>

Daher, M., R. Basar, E. Gokdemir, N. Baran, N. Uprety, A.K. Nunez Cortes, M. Mendt, L.N. Kerbauy, P.P. Banerjee, M. Shanley, et al. 2021. Targeting a cytokine checkpoint enhances the fitness of armored cord blood CAR-NK cells. *Blood.* 137:624–636. <https://doi.org/10.1182/blood.2020007748>

Delpoux, A., R.H. Michelini, S. Verma, C.-Y. Lai, K.D. Omilusik, D.T. Utzschneider, A.J. Redwood, A.W. Goldrath, C.A. Benedict, and S.M. Hedrick. 2018. Continuous activity of Foxo1 is required to prevent anergy and maintain the memory state of CD8⁺ T cells. *J. Exp. Med.* 215: 575–594. <https://doi.org/10.1084/jem.20170697>

Deng, Y., Y. Kerdiles, J. Chu, S. Yuan, Y. Wang, X. Chen, H. Mao, L. Zhang, J. Zhang, T. Hughes, et al. 2015. Transcription factor Foxo1 is a negative regulator of natural killer cell maturation and function. *Immunity.* 42:457–470. <https://doi.org/10.1016/j.immuni.2015.02.006>

Gartel, A.L., and A.L. Tyner. 2002. The role of the cyclin-dependent kinase inhibitor p21 in apoptosis. *Mol. Cancer Therapeut.* 1:639–649.

Goodridge, J.P., B. Jacobs, M.L. Saetersmoen, D. Clement, Q. Hammer, T. Clancy, E. Skarpen, A. Brech, J. Landskron, C. Grimm, et al. 2019. Remodeling of secretory lysosomes during education tunes functional potential in NK cells. *Nat. Commun.* 10:514. <https://doi.org/10.1038/s41467-019-08384-x>

Gordon, S.M., J. Chaix, L.J. Rupp, J. Wu, S. Madera, J.C. Sun, T. Lindsten, and S.L. Reinherz. 2012. The transcription factors T-bet and eomes control key checkpoints of natural killer cell maturation. *Immunity.* 36:55–67. <https://doi.org/10.1016/j.immuni.2011.11.016>

Hart, G.T., T.M. Tran, J. Theorell, H. Schlums, G. Arora, S. Rajagopalan, A.D.J. Sangala, K.J. Welsh, B. Traore, S.K. Pierce, et al. 2019. Adaptive NK cells in people exposed to plasmodium falciparum correlate with protection from malaria. *J. Exp. Med.* 216:1280–1290. <https://doi.org/10.1084/jem.20181681>

Hollyoake, M., R.D. Campbell, and B. Aguado. 2005. NKP30 (NCR3) is a pseudogene in 12 inbred and wild mouse strains, but an expressed gene in mus caroli. *Mol. Biol. Evol.* 22:1661–1672. <https://doi.org/10.1093/molbev/msi162>

Holmes, T.D., R.V. Pandey, E.Y. Helm, H. Schlums, H. Han, T.M. Campbell, T.T. Drashansky, S. Chiang, C.-Y. Wu, C. Tao, et al. 2021. The transcription factor Bcl11b promotes both canonical and adaptive NK cell differentiation. *Sci. Immunol.* 6:eabc9801. <https://doi.org/10.1126/sciimmunol.abc9801>

Jia, R., and J.S. Bonifacino. 2019. Lysosome positioning influences mTORC2 and AKT signaling. *Mol. Cell.* 75:26–38.e3. <https://doi.org/10.1016/j.molcel.2019.05.009>

Krämer, B., R. Knoll, L. Bonaguro, M. ToVinh, J. Raabe, R. Astaburuaga-García, J. Schulte-Schrepping, K.M. Kaiser, G.J. Rieke, J. Bischoff, et al. 2021. Early IFN- α signatures and persistent dysfunction are distinguishing features of NK cells in severe COVID-19. *Immunity.* 54: 2650–2669.e14. <https://doi.org/10.1016/j.immuni.2021.09.002>

Lanier, L.L. 2009. DAP10- and DAP12-associated receptors in innate immunity. *Immunol. Rev.* 227:150–160. <https://doi.org/10.1111/j.1600-065X.2008.00720.x>

- Lanier, L.L., B. Corliss, J. Wu, and J.H. Phillips. 1998. Association of DAP12 with activating CD94/NKG2C NK cell receptors. *Immunity*. 8:693-701. [https://doi.org/10.1016/S1074-7613\(00\)80574-9](https://doi.org/10.1016/S1074-7613(00)80574-9)
- Lanier, L.L., G. Yu, and J.H. Phillips. 1991. Analysis of Fc gamma RIII (CD16) membrane expression and association with CD3 zeta and Fc epsilon RI-gamma by site-directed mutation. *J. Immunol.* 146:1571-1576
- Lebrech, H., M.J. Horner, K.S. Gorski, W. Tsuji, D. Xia, W.-J. Pan, G. Means, G. Pietz, N. Li, M. Retter, et al. 2013. Homeostasis of human NK cells is not IL-15 dependent. *J. Immunol.* 191:5551-5558. <https://doi.org/10.4049/jimmunol.1301000>
- Lee, J., T. Zhang, I. Hwang, A. Kim, L. Nitschke, M. Kim, J.M. Scott, Y. Kamimura, L.L. Lanier, and S. Kim. 2015. Epigenetic modification and antibody-dependent expansion of memory-like NK cells in human cytomegalovirus-infected individuals. *Immunity*. 42:431-442. <https://doi.org/10.1016/j.immuni.2015.02.013>
- Liu, L.L., J. Landskron, E.H. Ask, M. Enqvist, E. Sohlberg, J.A. Traherne, Q. Hammer, J.P. Goodridge, S. Larsson, J. Jayaraman, et al. 2016. Critical role of CD2 Co-stimulation in adaptive natural killer cell responses revealed in NKG2C-deficient humans. *Cell Rep.* 15:1088-1099. <https://doi.org/10.1016/j.celrep.2016.04.005>
- Liu, W., J.M. Scott, E. Langguth, H. Chang, P.H. Park, and S. Kim. 2020. FcRγ gene editing reprograms conventional NK cells to display key features of adaptive human NK cells. *iScience*. 23:101709. <https://doi.org/10.1016/j.isci.2020.101709>
- Lopez-Vergès, S., J.M. Milush, S. Pandey, V.A. York, J. Arakawa-Hoyt, H. Pircher, P.J. Norris, D.F. Nixon, and L.L. Lanier. 2010. CD57 defines a functionally distinct population of mature NK cells in the human CD56dimCD16⁺ NK-cell subset. *Blood*. 116:3865-3874. <https://doi.org/10.1182/blood-2010-04-282301>
- Mace, E.M. 2018. Phosphoinositide-3-Kinase signaling in human natural killer cells: New insights from primary immunodeficiency. *Front. Immunol.* 9:445. <https://doi.org/10.3389/fimmu.2018.00445>
- Mao, Y., V. van Hoef, X. Zhang, E. Wennerberg, J. Lorent, K. Witt, L. Masvidal, S. Liang, S. Murray, O. Larsson, et al. 2016. IL-15 activates mTOR and primes stress-activated gene expression leading to prolonged antitumor capacity of NK cells. *Blood*. 128:1475-1489. <https://doi.org/10.1182/blood-2016-02-698027>
- Marçais, A., J. Cherfils-Vicini, C. Viant, S. Degouve, S. Viel, A. Fenis, J. Rabilloud, K. Mayol, A. Tavares, J. Bienvenu, et al. 2014. The metabolic checkpoint kinase mTOR is essential for IL-15 signaling during the development and activation of NK cells. *Nat. Immunol.* 15:749-757. <https://doi.org/10.1038/ni.2936>
- Marçais, A., M. Marotel, S. Degouve, A. Koenig, S. Fauteux-Daniel, A. Drouillard, H. Schlums, S. Viel, L. Besson, O. Allatif, et al. 2017. High mTOR activity is a hallmark of reactive natural killer cells and amplifies early signaling through activating receptors. *Elife*. 6:e26423. <https://doi.org/10.7554/eLife.26423>
- Maucourant, C., I. Filipovic, A. Ponzetta, S. Aleman, M. Cornillet, L. Hertwig, B. Strunz, A. Lentini, B. Reinius, D. Brownlie, et al. 2020. Natural killer cell immunotypes related to COVID-19 disease severity. *Sci. Immunol.* 5:eabd6832. <https://doi.org/10.1126/sciimmunol.abd6832>
- Merino, A.M., R.S. Mehta, X. Luo, H. Kim, T. De For, M. Janakiram, S. Cooley, R. Wangen, F. Cichocki, D.J. Weisdorf, et al. 2021. Early adaptive natural killer cell expansion is associated with decreased relapse after autologous transplantation for multiple myeloma. *Transplant. Cell Ther.* 27:310.e1-310.e6. <https://doi.org/10.1016/j.jtct.2020.10.023>
- Michelet, X., L. Dyck, A. Hogan, R.M. Loftus, D. Duquette, K. Wei, S. Beyaz, A. Tavakkoli, C. Foley, R. Donnelly, et al. 2018. Metabolic reprogramming of natural killer cells in obesity limits antitumor responses. *Nat. Immunol.* 19:1330-1340. <https://doi.org/10.1038/s41590-018-0251-7>
- Muccio, L., M. Falco, A. Bertaina, F. Locatelli, F. Frassoni, S. Sivori, L. Moretta, A. Moretta, and M. Della Chiesa. 2018. Late development of FcεRγneg adaptive natural killer cells upon human cytomegalovirus reactivation in umbilical cord blood transplantation recipients. *Front. Immunol.* 9:1050. <https://doi.org/10.3389/fimmu.2018.01050>
- Myers, D.R., E. Norlin, Y. Vercoulen, and J.P. Roose. 2019. Active tonic mTORC1 signals shape baseline translation in naive T cells. *Cell Rep.* 27:1858-1874.e6. <https://doi.org/10.1016/j.celrep.2019.04.037>
- Ohs, I., M. van den Broek, K. Nussbaum, C. Münz, S.J. Arnold, S.A. Quezada, S. Tugues, and B. Becher. 2016. Interleukin-12 bypasses common gamma-chain signalling in emergency natural killer cell lymphopoiesis. *Nat. Commun.* 7:13708. <https://doi.org/10.1038/ncomms13708>
- Ouyang, W., and M.O. Li. 2011. Foxo: In command of T lymphocyte homeostasis and tolerance. *Trends Immunol.* 32:26-33. <https://doi.org/10.1016/j.it.2010.10.005>
- Pahl, J.H.W., J. Koch, J.-J. Götz, A. Arnold, U. Reusch, T. Gantke, E. Rajkovic, M. Treder, and A. Cerwenka. 2018. CD16A activation of NK cells promotes NK cell proliferation and memory-like cytotoxicity against cancer cells. *Cancer Immunol. Res.* 6:517-527. <https://doi.org/10.1158/2326-6066.CIR-17-0550>
- Platanias, L.C. 2005. Mechanisms of type-I- and type-II-interferon-mediated signalling. *Nat. Rev. Immunol.* 5:375-386. <https://doi.org/10.1038/nri1604>
- Rao, R.R., Q. Li, M.R. Bupp, and P.A. Shrikant. 2012. Transcription factor Foxo1 represses T-bet-mediated effector functions and promotes memory CD8⁺ T cell differentiation. *Immunity*. 36:374-387. <https://doi.org/10.1016/j.immuni.2012.01.015>
- Rölle, A., M. Meyer, S. Calderazzo, D. Jäger, and F. Momburg. 2018. Distinct HLA-E peptide complexes modify antibody-driven effector functions of adaptive NK cells. *Cell Rep.* 24:1967-1976.e4. <https://doi.org/10.1016/j.celrep.2018.07.069>
- Romee, R., M. Rosario, M.M. Berrien-Elliott, J.A. Wagner, B.A. Jewell, T. Schappe, J.W. Leong, S. Abdel-Latif, S.E. Schneider, S. Willey, et al. 2016. Cytokine-induced memory-like natural killer cells exhibit enhanced responses against myeloid leukemia. *Sci. Transl. Med.* 8:357ra123. <https://doi.org/10.1126/scitranslmed.aaf2341>
- Rozengurt, E., H.P. Soares, and J. Sinnett-Smith. 2014. Suppression of feedback loops mediated by PI3K/mTOR induces multiple over-activation of compensatory pathways: An unintended consequence leading to drug resistance. *Mol. Cancer Therapeut.* 13:2477-2488. <https://doi.org/10.1158/1535-7163.MCT-14-0330>
- Sarbasov, D.D., S.M. Ali, S. Sengupta, J.-H. Sheen, P.P. Hsu, A.F. Bagley, A.L. Markhard, and D.M. Sabatini. 2006. Prolonged rapamycin treatment inhibits mTORC2 assembly and akt/PKB. *Mol. Cell.* 22:159-168. <https://doi.org/10.1016/j.molcel.2006.03.029>
- Schlums, H., F. Cichocki, B. Tesi, J. Theorell, V. Beziat, T.D. Holmes, H. Han, S.C.C. Chiang, B. Foley, K. Mattsson, et al. 2015. Cytomegalovirus infection drives adaptive epigenetic diversification of NK cells with altered signaling and effector function. *Immunity*. 42:443-456. <https://doi.org/10.1016/j.immuni.2015.02.008>
- Shah, S.V., C. Manickam, D.R. Ram, K. Kroll, H. Itell, S.R. Permar, D.H. Barouch, N.R. Klatt, and R.K. Reeves. 2018. CMV primes functional alternative signaling in adaptive Δg NK cells but is subverted by lentiviral infection in Rhesus macaques. *Cell Rep.* 25:2766-2774.e3. <https://doi.org/10.1016/j.celrep.2018.11.020>
- Shemesh, A., H. Pickering, K.T. Roybal, and L.L. Lanier. 2022. Differential IL-12 signaling induces human natural killer cell activating receptor-mediated ligand-specific expansion. *J. Exp. Med.* 219:e20212434. <https://doi.org/10.1084/jem.20212434>
- Staron, M.M., S.M. Gray, H.D. Marshall, I.A. Parish, J.H. Chen, C.J. Perry, G. Cui, M.O. Li, and S.M. Kaech. 2014. The transcription factor FoxO1 sustains expression of the inhibitory receptor PD-1 and survival of antiviral CD8(+) T cells during chronic infection. *Immunity*. 41:802-814. <https://doi.org/10.1016/j.immuni.2014.10.013>
- Steinbach, K., I. Vincenti, and D. Merkler. 2018. Resident-memory T cells in tissue-restricted immune responses: For better or worse?. *Front. Immunol.* 9:2827. <https://doi.org/10.3389/fimmu.2018.02827>
- Su, Y., D. Chen, D. Yuan, C. Lausted, J. Choi, C.L. Dai, V. Voillet, V.R. Duvvuri, K. Scherler, P. Troisch, et al. 2020. Multi-omics resolves a sharp disease-state shift between mild and moderate COVID-19. *Cell*. 183:1479-1495.e20. <https://doi.org/10.1016/j.cell.2020.10.037>
- Sun, J.C., J.N. Beilke, N.A. Bezman, and L.L. Lanier. 2011. Homeostatic proliferation generates long-lived natural killer cells that respond against viral infection. *J. Exp. Med.* 208:357-368. <https://doi.org/10.1084/jem.20100479>
- Sun, J.C., J.N. Beilke, and L.L. Lanier. 2009. Adaptive immune features of natural killer cells. *Nature*. 457:557-561. <https://doi.org/10.1038/nature07665>
- Takahashi, K., N. Hayashi, T. Shimokawa, N. Umehara, S. Kaminogawa, and C. Ra. 2008. Cooperative regulation of Fc receptor γ-chain gene expression by multiple transcription factors, including Sp1, GABP, and Elf-1. *J. Biol. Chem.* 283:15134-15141. <https://doi.org/10.1074/jbc.M800498200>
- Tao, L., and T.A. Reese. 2017. Making mouse models that reflect human immune responses. *Trends Immunol.* 38:181-193. <https://doi.org/10.1016/j.it.2016.12.007>
- Tapias, A., C.J. Ciudad, I.B. Roninson, and V. Noé. 2008. Regulation of Sp1 by cell cycle related proteins. *Cell Cycle*. 7:2856-2867. <https://doi.org/10.4161/cc.7.18.6671>

- Varchetta, S., D. Mele, B. Oliviero, S. Mantovani, S. Ludovisi, A. Cerino, R. Bruno, A. Castelli, M. Mosconi, M. Vecchia, et al. 2021. Unique immunological profile in patients with COVID-19. *Cell Mol. Immunol.* 18: 604–612. <https://doi.org/10.1038/s41423-020-00557-9>
- Viant, C., S. Guia, R.J. Hennessy, J. Rautela, K. Pham, C. Bernat, W. Goh, Y. Jiao, R. Delconte, M. Roger, et al. 2017. Cell cycle progression dictates the requirement for BCL2 in natural killer cell survival. *J. Exp. Med.* 214: 491–510. <https://doi.org/10.1084/jem.20160869>
- Viel, S., A. Marçais, F.S.-F. Guimaraes, R. Loftus, J. Rabilloud, M. Grau, S. Degouve, S. Djebali, A. Sanlaville, E. Charrier, et al. 2016. TGF- β inhibits the activation and functions of NK cells by repressing the mTOR pathway. *Sci. Signal.* 9:ra19. <https://doi.org/10.1126/scisignal.aad1884>
- Walk, J., and R.W. Sauerwein. 2019. Activatory receptor Nkp30 predicts NK cell activation during controlled human malaria infection. *Front. Immunol.* 10:2864. <https://doi.org/10.3389/fimmu.2019.02864>
- Wang, F., M. Meng, B. Mo, Y. Yang, Y. Ji, P. Huang, W. Lai, X. Pan, T. You, H. Luo, et al. 2018. Crosstalks between mTORC1 and mTORC2 variagate cytokine signaling to control NK maturation and effector function. *Nat. Commun.* 9:4874. <https://doi.org/10.1038/s41467-018-07277-9>
- Wang, X., and X.-Y. Zhao. 2021. Transcription factors associated with IL-15 cytokine signaling during NK cell development. *Front. Immunol.* 12: 610789. <https://doi.org/10.3389/fimmu.2021.610789>
- Wiedemann, G.M., S. Grassmann, C.M. Lau, M. Rapp, A.V. Villarino, C. Friedrich, G. Gasteiger, J.J. O’Shea, and J.C. Sun. 2020. Divergent role for STAT5 in the adaptive responses of natural killer cells. *Cell Rep.* 33: 108498. <https://doi.org/10.1016/j.celrep.2020.108498>
- Wiedemann, G.M., E.K. Santosa, S. Grassmann, S. Sheppard, J.-B. Le Luque, N.M. Adams, C. Dang, K.C. Hsu, J.C. Sun, and C.M. Lau. 2021. Deconvoluting global cytokine signaling networks in natural killer cells. *Nat. Immunol.* 22:627–638. <https://doi.org/10.1038/s41590-021-00909-1>
- Witkowski, M., C. Tizian, M. Ferreira-Gomes, D. Niemeyer, T.C. Jones, F. Heinrich, S. Frischbutter, S. Angermair, T. Hohnstein, I. Mattioli, et al. 2021. Untimely TGF β responses in COVID-19 limit antiviral functions of NK cells. *Nature.* 600:295–301. <https://doi.org/10.1038/s41586-021-04142-6>
- Wu, Z., C. Sinzger, G. Frascaroli, J. Reichel, C. Bayer, L. Wang, R. Schirmbeck, and T. Mertens. 2013. Human cytomegalovirus-induced NKG2Chi CD57hi natural killer cells are effectors dependent on humoral antiviral immunity. *J. Virol.* 87:7717–7725. <https://doi.org/10.1128/JVI.01096-13>
- Yang, C., S.-W. Tsaih, A. Lemke, M.J. Flister, M.S. Thakar, and S. Malarkannan. 2018. mTORC1 and mTORC2 differentially promote natural killer cell development. *Elife.* 7:e35619. <https://doi.org/10.7554/eLife.35619>
- Yang, G., D.S. Murashige, S.J. Humphrey, and D.E. James. 2015. A positive feedback loop between akt and mTORC2 via SIN1 phosphorylation. *Cell Rep.* 12:937–943. <https://doi.org/10.1016/j.celrep.2015.07.016>
- Yu, Y., M. Wang, X. Zhang, S. Li, Q. Lu, H. Zeng, H. Hou, H. Li, M. Zhang, F. Jiang, et al. 2021. Antibody-dependent cellular cytotoxicity response to SARS-CoV-2 in COVID-19 patients. *Signal Transduct. Targeted Ther.* 6: 346. <https://doi.org/10.1038/s41392-021-00759-1>
- Zaghi, E., M. Calvi, S. Puccio, G. Spata, S. Terzoli, C. Peano, A. Roberto, F. De Paoli, J.J. van Beek, J. Mariotti, et al. 2021. Single-cell profiling identifies impaired adaptive NK cells expanded after HCMV reactivation in haploidentical HSCT. *JCI Insight.* 6:e146973. <https://doi.org/10.1172/jci.insight.146973>
- Zhang, J., M. Marotel, S. Fauteux-Daniel, A.-L. Mathieu, S. Viel, A. Marçais, and T. Walzer. 2018. T-bet and Eomes govern differentiation and function of mouse and human NK cells and ILC1. *Eur. J. Immunol.* 48: 738–750. <https://doi.org/10.1002/eji.201747299>
- Zhang, L., B.O. Tschumi, I.C. Lopez-Mejia, S.G. Oberle, M. Meyer, G. Samson, M.A. Ruegg, M.N. Hall, L. Fajas, D. Zehn, et al. 2016. Mammalian target of rapamycin complex 2 controls CD8 T cell memory differentiation in a Foxo1-dependent manner. *Cell Rep.* 14:1206–1217. <https://doi.org/10.1016/j.celrep.2015.12.095>
- Zhuang, X., D.P. Veltri, and E.O. Long. 2019. Genome-wide CRISPR screen reveals cancer cell resistance to NK cells induced by NK-derived IFN- γ . *Front. Immunol.* 10:2879. <https://doi.org/10.3389/fimmu.2019.02879>

Supplemental material

A Patients' information

Subject	Transplant indication	Sex	Age	Medications at baseline	Sirolimus indication	Medications post-sirolimus	Sirolimus trough (ug/liter)	HCMV status
Patient #1	ILD	F	57	T, MMF, P	CKD	T, P, sirolimus	6.7	R+/DU
Patient #2	ILD	F	55	T, MMF, P	CLAD	T, P, sirolimus	11.1	R-/D-
Patient #3	ILD	M	50	T, MMF, P	ACR	T, P, sirolimus	6.3	R-/D-
Patient #4	ILD	M	69	T, MMF, P	CKD	T, P, sirolimus	7.1	R-/D-
Control A	ILD	M	45	T, MMF, P				R+/D+
Control B	ILD	M	59	T, MMF, P				R+/D+
Control C	ILD	M	64	T, MMF, P				R+/D+
Control D	ILD	M	40	T, MMF, P				R+/DU
Control E	ILD	F	58	T, MMF, P				R+/D+

Abbreviations:

ILD, interstitial lung disease; M, male; F, female; T, tacrolimus; MMF, mycophenolate mofetil; P, prednisone; CKD, chronic kidney disease; CLAD, chronic lung allograft dysfunction; ACR, acute cellular rejection, R = recipient, D = donor, DU = donor unknown, HCMV status = CMV serology

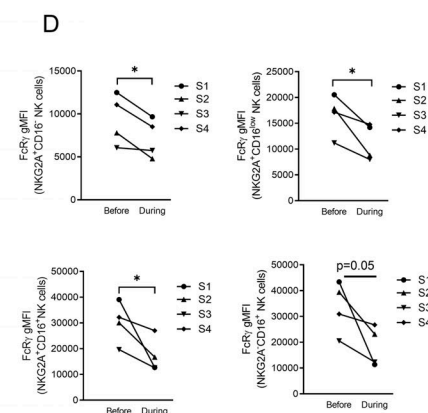
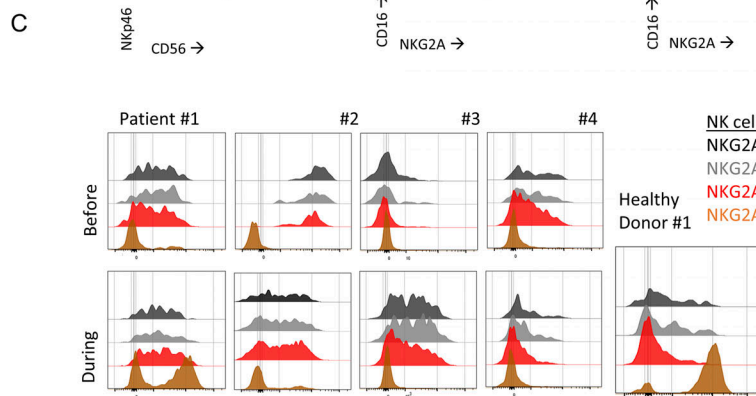
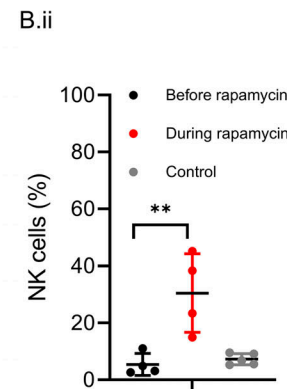
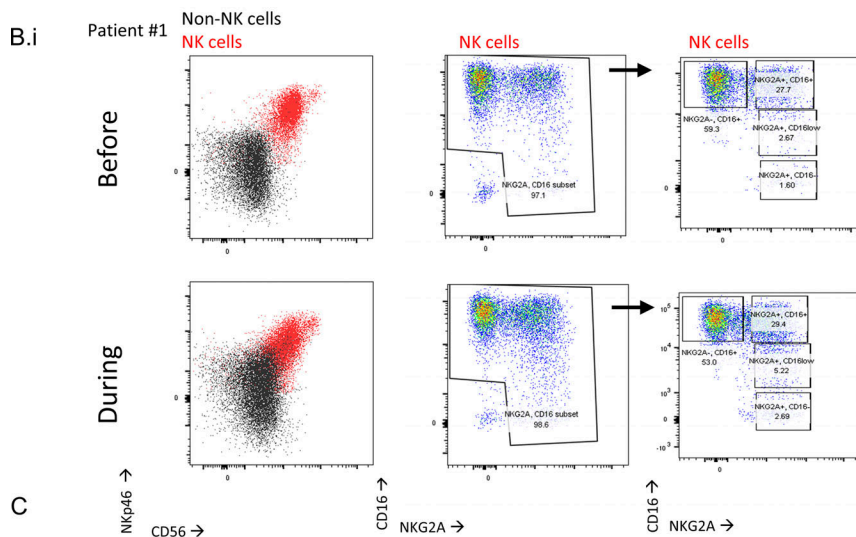


Figure S1. Lung transplant patients' clinical information, and NK cell percentages and markers. (A) Lung transplant patients' clinical status. (B i) Representative flow cytometry gating analysis of matched samples from lung transplant recipients before (upper panels) or during (lower panels) rapamycin treatment. NK cells were identified as live CD45⁺NKp46⁺CD3⁻, CD19⁻, CD14⁻, CD123⁻, and CD4⁻ cells, and subgated by NKG2A versus CD16 expression. (B ii) Percentages of NK cells of CD45⁺ cells. Mean ± SD, one tail, **, P < 0.01. (C) Histograms of NKG2C expression in the defined NK cell subsets for each patient before or during rapamycin treatment. (D) FcRγ levels in specified NK cell subsets before or during rapamycin treatment per patient. Paired t test, one tail, *, P ≤ 0.05.

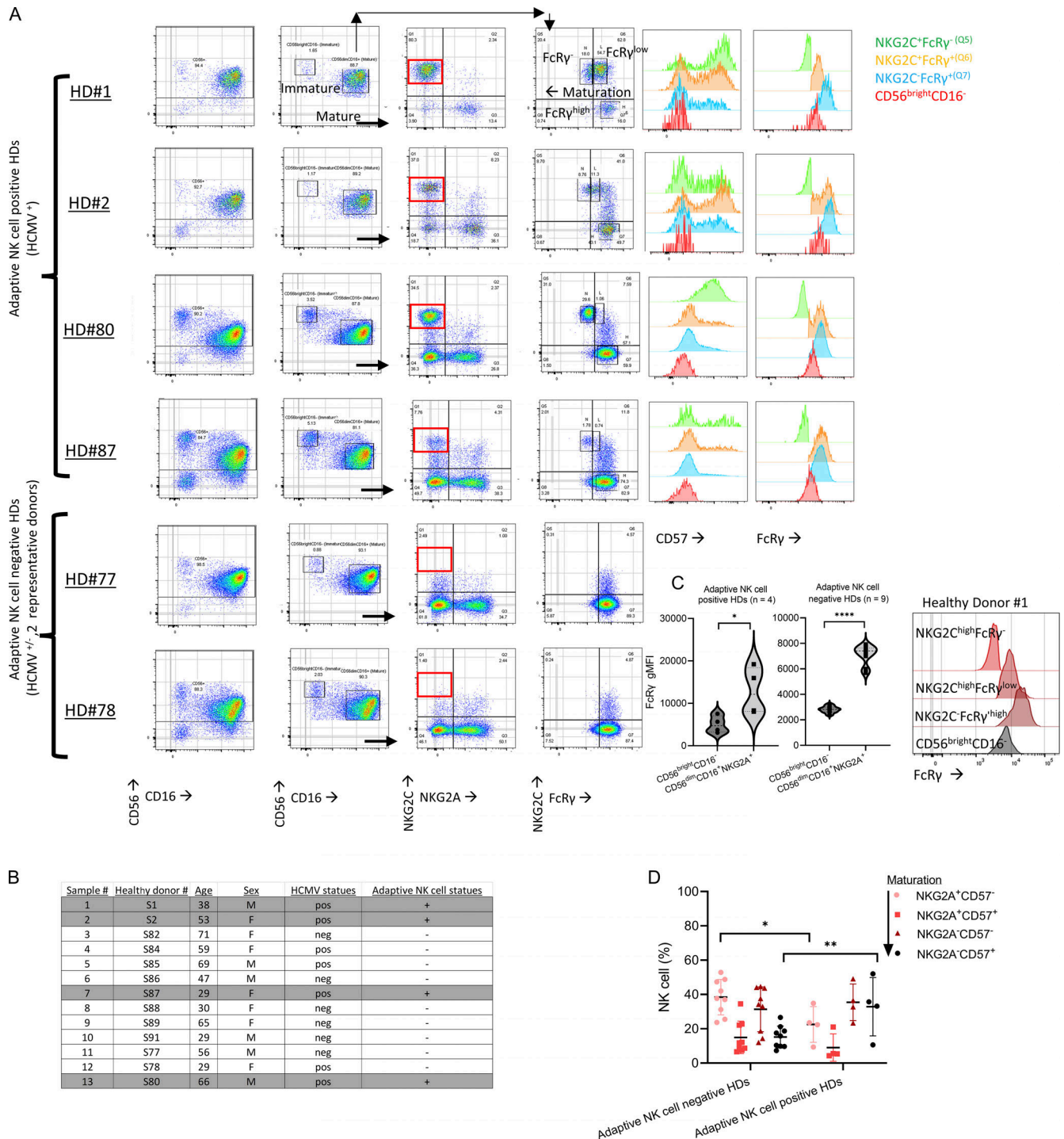


Figure S2. **Healthy donors NK cell gating strategy and donors' information.** (A) Representative dot plots showing gating of CD56^{bright}CD16⁻, CD56^{dim}CD16⁺, expression of NKG2C vs. NKG2A and NKG2C vs. FcRy in CD56^{dim}CD16⁺ cells, and CD57 expression in the defined NK cell subsets. HD #1, #2, #80, #87: adaptive NK cell-positive HDs. HD #77 and HD #78 represent adaptive NK cell-negative HDs (without NKG2C^{high} or FcRy^{-/low} mature adaptive NK cells). (B) HDs' age, sex, HCMV statuses, and adaptive NK cell statuses. (C) Expression of FcRy protein in CD56^{bright}CD16⁻ relative to CD56^{dim}CD16⁺NKG2A⁺ NK cells in adaptive NK cell-positive or -negative HDs. Right: Representative histograms of FcRy expression in immature CD56^{bright}CD16⁻ NK cells relative to mature NK cell subsets defined by NKG2C and FcRy expression (Fig. S2 A). Paired t-test, parametric. *, P ≤ 0.05; ****, P < 0.0001. (D) Comparison of the percentages of NK cell subsets defined by NK cell maturation (NKG2A⁺CD57⁻ → NKG2A⁻CD57⁺) between adaptive NK cell-negative or -positive donors' groups. Mean ± SD, unpaired t test, two tails, *, P < 0.05; **, P < 0.01.

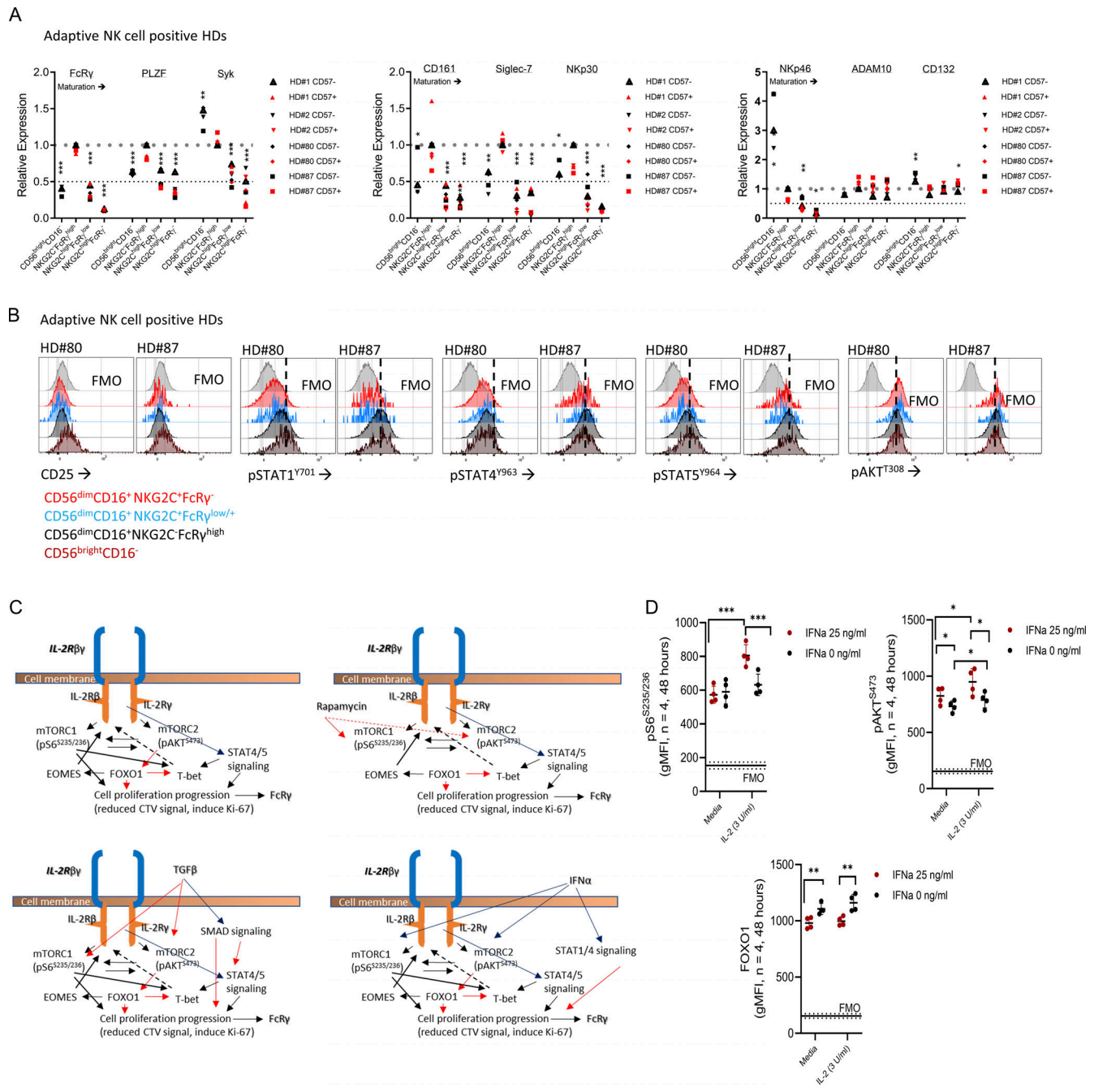


Figure S3. Characterization of ex vivo primary adaptive NK cells. (A) Relative expression of adaptive NK cell-associated markers (FcRy, PLZF, Syk, CD161, siglec-7, Nkp30, and Nkp46) or the metalloproteinase ADAM10 (reported to cleave CD122), or CD132 (IL-2Ry) in the defined NK cell subsets from adaptive NK cell-positive HDs. Paired t test, parametric. *, $P < 0.05$; **, $P < 0.01$; ***, $P < 0.001$ (index = 1 [upper dashed line], index = 0.5 [lower dashed line]). Statistical calculation was performed relative to NKG2C⁻FcRy^{high} NK cells. **(B)** Representative histograms for CD25 (IL-2R α), pSTAT1, pSTAT4, pSTAT5, and pAKT^{T308} expression in CD56^{bright}CD16⁻ and the specified CD56^{dim}CD16⁺ NK cell subsets, ex vivo (FMO = fluorescence minus one control). **(C)** Schematic representation of signaling pathways involved in FcRy regulation according to experiments preformed. Upper panels: Left, IL-2 or IL-15 stimulation; right, IL-2 or IL-15 stimulation and rapamycin. Lower panels: Left, IL-2 or IL-15 stimulation and TGF β ; right, IL-2 or IL-15 stimulation and IFN α . Black line \rightarrow activation, red line \rightarrow suppression, solid line \rightarrow strong, dashed line \rightarrow weak. **(D)** mTORC1 activity, mTORC2 activity, and FOXO1 protein levels following 48 h of the indicated IFN α stimulation. Paired t test, parametric. *, $P < 0.05$; **, $P < 0.01$; ***, $P < 0.001$. Horizontal dashed line = FMO control values.

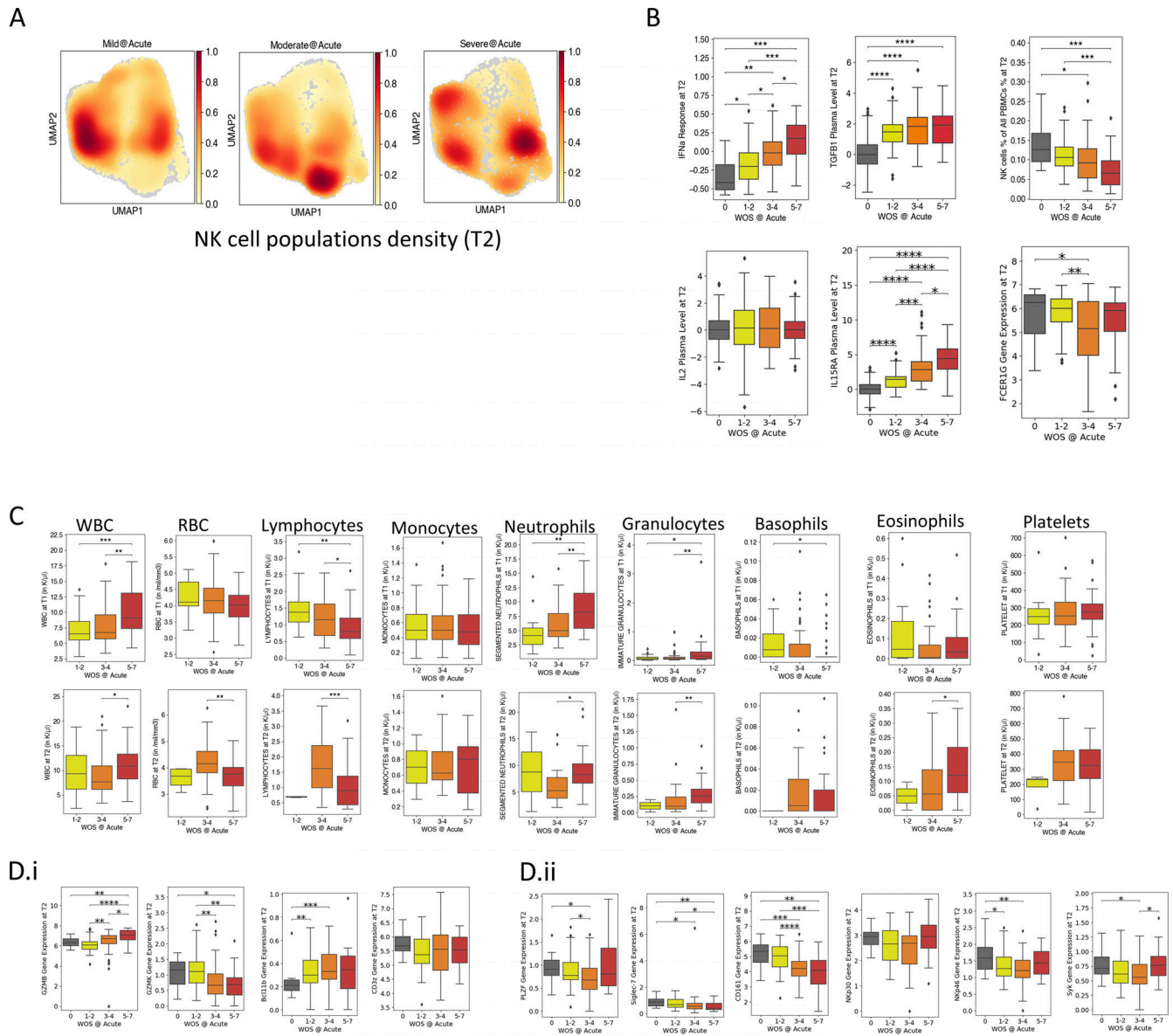


Figure S4. Characterization of COVID-19 blood samples. (A) Complementary UMAPs of NK cell population density by gene expression subdivided by WOS score: mild (1–2), moderate (3–4), and severe (5–6) in acute (T2) samples. (B) Upper panels (left to right): IFN α response transcriptomic signature score in NK cells, TGF β levels in plasma, NK cell percentages with in all PBMCs. Lower panels (left to right): IL-2 levels in plasma, IL-15Ra levels in plasma, and FcR γ gene expression within all NK cells, across patients with different WOS COVID-19 disease severity score in acute (T2) stages. (C) Counts per K/ μ l of the indicated cell types at baseline T1 (upper panels) and acute T2 timepoints (lower panels). (D) Maturation-associated markers (left to right: GZMB, GZMK, and Bcl11b) and CD3 ζ gene expression (i), and adaptive NK cell-associated markers (left to right: PLZF, Siglec-7, CD161, NKp30, NKp46, and Syk; ii) within the NK cell population across patients with different WOS COVID-19 disease severity score in acute stage (T2). Mann Whitney U test, *, $P < 0.05$; **, $P < 0.01$; ***, $P < 0.001$; ****, $P < 0.0001$.

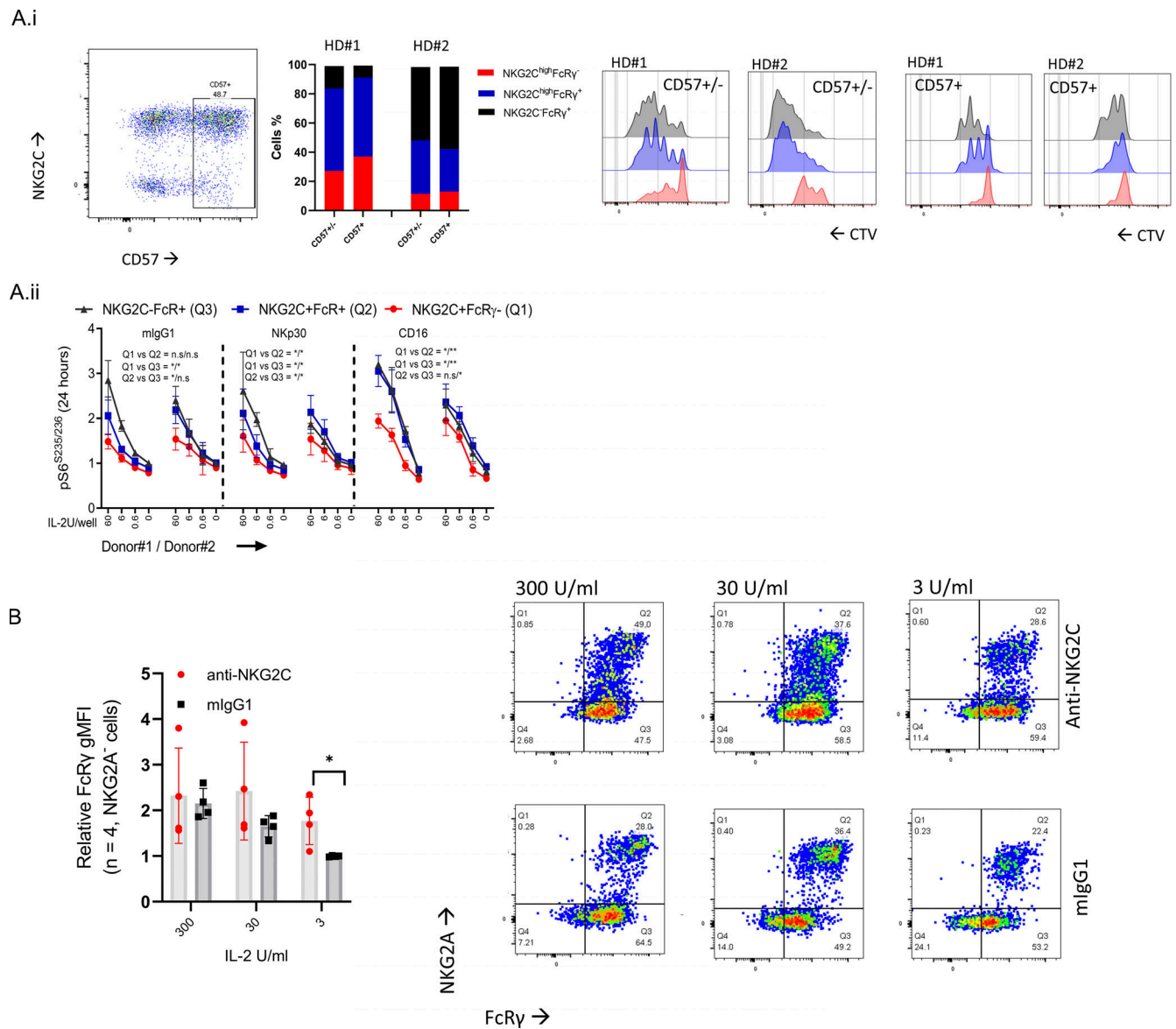


Figure S5. **Influence of CD16 or NKG2C stimulation on adoptive FcRy^{-/low} NK cells.** (A i) NK cell proliferation (CTV assay) of sorted CD57⁺ vs. unsorted CD57⁺ adaptive vs. nonadaptive NK cells from HDs #1, #2 after stimulation with anti-CD16 + IL-2 (6 U/ml). (A ii) Normalized pS6 gMFI levels after 24 h of the indicate stimulation in the defined mature NK cell subsets. Mean \pm SD. Paired *t* test, two tails, *, *P* < 0.05; **, *P* < 0.01. (B) FcRy levels of NKG2A⁻ NK cells in donors with adoptive NK cells (Fig. S2). Cells were stimulated with anti-NKG2C-coated or mouse IgG1 isotype-matched control-coated beads for 6 d in the presence of increasing IL-2 concentrations. Mean \pm SD. Paired *t* test, parametric. *, *P* < 0.05.